HYDROMECHANICAL MODEL OF THE MOVEMENT OF FLOATING, AGGREGATED DEFORMABLE BODIES

By

ROYANN J PETRELL

A DISSERTATION PRESENTED TO THE GRADUATE SCHOOL
OF THE UNIVERSITY OF FLORIDA IN
PARTIAL FULFILLMENT OF THE REQUIREMENTS
FOR THE DEGREE OF DOCTOR OF PHILOSOPHY

UNIVERSITY OF FLORIDA

1988

ACKNOWLEDGMENTS

The author is indebted to Dr. Larry O. Bagnall, her major professor, for his support, encouragement, advice and assistance throughout the course of this work.

The author is also grateful to Dr. Glen H. Smerage, Dr. Del Bottcher, Dr. Chang T. Sun, and Dr. Wayne Mishoe for their advice and time. Appreciation is extended to the Civil Engineering Department for the use of the hydraulics laboratory and to R. A. Christensen and E. Dobson for their help there.

The author is very grateful to Mike Simpson, Jorge Sosa, Manuel Almeda, and her sister Janet Petrali for their sense of adventure, courage and strength, and for their help with the water hyacinth experiments.

Finally, the author appreciates deeply the constant support and encouragement from her husband Alfredo Rodriguez, and the patience of her family and friends.

TABLE OF CONTENTS

KEY TO SYMBOLS

English Symbols

a	characteristic length
a'	semi-contact widths
A	area
A_r	projected flow area of a rhizome = $D_r L_r$
A_s	specific mat area = A_t / M_p
A_t	mat area as a function of time
b	roughness element width
B_L	interactive plant friction coefficient
C	Chezy discharge coefficients $1/n\ R^{1/6}$
C_d	drag coeficient
C_e	experimental proportionality constant= $1000\ N_p\ A_r\ C_d$
C_1 C_2	experimental constants for flow in vegetated channel
d	deviation of actual value from computed value
D_c	maximum expected mat compaction value- m
D_f	drag force
D_r	rhizome diameter

D_v	constant used to determine unsteady drag coefficient
e	transverse spacing length of roughness element
E	Young's elastic modulus
F	friction factor for crossflow over a bank of cylinders
F_c	sliding friction contact force
F_k	elastic force
F_M	inertia
g	acceleration due to gravity
G	mass flow rate
h	roughness element height
I	moment of inertia
k_s	height of grain for equivalent sand roughness
K	elastic constant
$\mathcal{L}$	flow length
ℓ	cantilever beam length
L_r	rhizome length
L	initial mat length
L'	variable used to determine unsteady drag coefficient
m	Reynolds number exponent
M	mass
M_p	total mass of plants in a mat
n	Manning's roughness coefficient
N	statistical sample size
N_p	number of plants in a mat
p	number of major restrictions encountered by flow through a bank of cylinders

P	applied load
q	statistical number used for determination of spurious errors
r	cylinder radius
R	hydraulic radius
S_c	standard error of coefficient
S_e	standard error of estimate
v	deformation of diametrical mid section of a cylinder
V	velocity of body relative to undisturbed fluid
V_*	friction velocity = $\sqrt{\tau_o/\rho}$
w	normal approach of a flat plate to the center of a cylinder
W	bar width
x	longitudinal spacing of roughness baffle
X	spatial displacement
Y	half-angle of contact between a clinder and a flat plate
y_n	normal depth of flow

Greek Symbols

δ	deflections or deformation
ν	kinematic viscosity
ρ	density
τ_o	shearing stress at a wall
φ	Poisson's ratio
ω_n	natural frequency

Abstract of Dissertation Presented to the Graduate School
of the University of Florida in Partial Fulfillment of the
Requirements for the Degree of Doctor of Philosophy

HYDROMECHANICAL MODEL OF THE MOVEMENT OF FLOATING
AGGREGATED DEFORMABLE BODIES

By

Reyann J. Petrell

December 1988

Chairman: Larry O. Bagnall and J. Wayne Mishoe
Major Department: Agricultural Engineering

In this study, complicated machine plant interactions were analyzed so that more efficient harvesters could be designed. Plants investigated were water hyacinths (*Eichhornia crassipes*), which are floating hydrophytes that grow together to form mats or aggregates. Because mechanical harvesting is expensive and time consuming, they are currently harvested to control their propagation in water bodies only where a chemical or biological method is prohibited or unsuccessful. More efficient harvesting methods will depend on equipment designs based on hydromechanical characteristics of mats, which up to now have been inadequately known to predict performance of towing or removal systems.

Conceptual models were developed that describe machine water hyacinth interactions for two different harvesting operations rectangular mat towing and forced compaction. The mathematical description of mats was based on experimental observations and physical and hydromechanical principles. Primary system variables are horizontal displacement and velocity of the mat, and the input variable is either towing or compaction velocity as a function of time.

Equations derived from the conceptual models were solved numerically, and output variables such as compacting and towing forces, mat instability, and change in mat length, were predicted over time with good correlation with experimental data. Mat drag coefficient was found to be independent of Reynolds number but dependent on mat geometry. Power input to harvesters can be reduced by careful selection of acceleration patterns, towing or compaction velocity, mat geometry, and standing plant densities.

CHAPTER I
INTRODUCTION

Water hyacinths (Eichhornia crassipes) are free-floating emergent hydrophytes or, in mechanical terms, deformable bodies that are positively buoyant. These plants grow together to form a mat or aggregate, and they are harvested to control their propagation in natural waterways, canals and some sewage treatment systems. In Florida, water hyacinths were eighth in acreage of all aquatic plants surveyed in 1986, and they are pests because they clog waterways (Schardt, 1986). Florida's Surface Water Improvement and Management Act (1987) includes aquatic plant management strategies to restore water bodies. Additional restrictions on pesticide use by the Environmental Protection Agency and the U. S. Fish and Wildlife Service will soon apply to herbicides used within ranges of protected plants and animals (Ramey, 1987). These political issues and increased use of water hyacinths in water treatment systems stress the importance of the development of efficient and fast ways to manage aquatic plants without the use of heavy, expensive mechanical equipment or potentially dangerous toxins and without the time delay often found in biological control methods.

The current cost to mechanically harvest water hyacinths is three to five dollars per wet ton (Bagnall et al., 1987). Typically, 200

tons of plants are found in one hectare, consequently the cost to harvest one hectare is \$600 to \$1000. On the other hand, chemical treatment costs approximately \$100/ha. The U.S. Army Corps of Engineers considers a system which harvests and disposes of 80 to 100 tons per hour to be efficient enough to control known growth rates of the water hyacinth (Culpepper and Decell, 1978). The Corps also found that the most advanced harvesting system available can not meet these conditions, and that the principal problem is the transportation of the plants over the water. For instance, one way of transportation is towing a mat of plants. Often, however, when a mat is towed, the plants tend to jam. Bogart (1949) described the mechanism of jam formation as a combination of accretion of plants and a rolling under action that increases the vertical dimensions of the mat. As a consequence of a jam, towing force increases, and occasionally a mat rolls under the containment device and escapes.

An efficient hyacinth harvester, thus, depends on simple equipment that is based on hydromechanical characteristics (e.g., drag forces and the elastic properties) of water hyacinth mats; however, physical characterization of aquatic plants has been inadequate to predict the performance of large towing or removal systems. The purpose of this research was to determine hydromechanical properties of water hyacinths necessary to predict the response of a water hyacinth mat to various force or velocity inputs and boundary restraints.

CHAPTER II
OBJECTIVES

The principle objectives of this research are listed below and each objective will be the focus of a subsequent chapter

-Quantitatively describe those physical characteristics of water hyacinth mats that distinguish one type of aggregation from another.

-Determine the hydrodynamic and elastic contact properties of water hyacinths, and find the equations that describe the relationships between viscous forces on mats and towing velocity and between contact forces and plant displacement within the mat

-Develop, from developed constitutive relations and structural equations, a mathematical model that predicts how a particular aggregation of water hyacinths reacts to an applied velocity.

-Validate the model and demonstrate practical applications for it

CHAPTER III
PHYSICAL CHARACTERISTICS OF WATER HYACINTH
ACCRECATIONS

Several physical characteristics of individual water hyacinth plants and of different aggregations are described in this chapter standing density, plant mass and structure, mat buoyancy and connectivity. The latter is a new property. Generally, these characteristics vary according to habitat, season and plant age, and affect harvest operations.

First, the morpho-anatomical description of water hyacinths provides expected ranges of plant mass, leaf, root, and rhizome length and diameters, and the internal cellular structure of the plants. This information is basic for the determination of inertia (e.g., plant mass) and for the identification of the plant parts that physically interact with water or with other plants.

The shapes of rhizomes and roots, the principal plant parts projecting into the water, influence the viscous forces generated when the plants are towed. An empirical method to predict rhizome lengths from other physical descriptions would be useful. Rhizomes are difficult to measure, because they are usually heavily covered with roots and debris.

Standing biomass density, in combination with harvesting speed and width, determines the capacity of a harvester and the power requirements for conveying or transportation systems. Also, plant mass affects inertial forces encountered in a towing operation. On the other hand, areal population density is useful in flow models because total projected area in flow depends on the number of plants. The measurement of areal population density is time consuming because it requires handling every plant; yet, an empirical method to predict population density from other physical description (e.g. plant mass or length) does not exist.

Mat buoyancy, the force required to submerge a given area of water hyacinths, is useful for the design of conveyors, booms and containment structures, since the plants under certain conditions roll under such devices. Water hyacinth plants can be connected through leaf entanglements and stolons. Mats have been characterized by either standing population or biomass density and, to a limited extent, by buoyancy, but the literature reports no property that would quantify the "connectiveness" of a mat; therefore, a test described in this chapter was developed to measure mat connectivity. Information on connectivity is needed when a mat is to be separated into smaller units for towing or lifting from the water. Also, information on connectivity changes could be useful in biological studies. Rapid decreases in connectivity in a mat could indicate that the plants have been subjected to physiological stresses.

The objectives of this chapter are:

-State from available literature the structure and composition of water hyacinths.

-Determine the distribution of mass in a water hyacinth aggregation and how that distribution could vary from one population to another

-Develop a relation between standing density and average plant size of a mat

-Develop an empirical method to calculate rhizome length.

-Determine how mat buoyancy varies for different mats, and find a relation with the use of plant size characteristics to predict it

-Determine connectivity for different mat types

Review of Literature.

Morpho-anatomical Description of the Water Hyacinth.

The mature water hyacinth plant is a free-floating (usually) emergent hydrophyte that consists of roots, rhizomes, stolons, leaves, inflorescence and fruit clusters (Figure 3.0). In limiting nutrient conditions, shoot to root length ratio in the range of 1-2 is common and 53% of the total plant dry matter is in the leaves and petiole. In nutrient-rich conditions, shoot to root ratios are in the range of 4-6, and up to 85% of the dry matter is in the foliage (Reddy, 1988). Medium-sized water hyacinths (500-2000 g/m^2 dw) are harvested free sewage treatment plants because plant densities are optimum for achieving maximum biomass yields (Reddy, 1988).

The fibrous root (as opposed to a tap root) has a dense cluster of main and lateral roots. The lateral roots are not randomly dispersed, and they are arranged in groups along the main root axes (Mallory et al., 1970). The roots of plants from different habitats and seasons vary little in diameter but can vary greatly in length. The diameter varies from 0.4 to 1.5 mm. The length varies from 4 to

Figure 3.0 A water hyacinth consists of leaves, roots, a rhizome, and stolons.

15 cm in small plants, 10 to 36 cm in medium plants, and 12 to 22 cm in large plants (Penfound and Earle, 1948 and Zamora et al., 1982).

A root has distinct regions: epidermis, cortex and stele. The epidermal cells are either oblong, square or rectangular in shape and are 40 to 80 μm in size. The cortical regions consist of an outer layer of parenchyma cells, a cortical lacunae that covers 7/10 of the cortex, an inner layer of parenchyma cells, and an endodermis that measures 2/10 of the cortex. The stele consists of a xylem region, 10 to 13 layers of parenchyma cells, and 10 to 15 cells of phloem (Zamora et al., 1982).

A rhizome is a stem or axis with short internodes. The rhizome produces at the numerous nodes all the roots, leaves, offshoots, and inflorescences of the plant. The diameter of the stem varies from 1 to 3 cm and the length from 1 to 30 cm. Structurally similar to a root, a rhizome consists of epidermal, cortical and stele regions. The stele contains very few fibers, but some tracheary elements are present which increase in number and size as the rhizome matures. The cortical region consists of parenchyma tissue and air spaces (Zamora et al., 1980).

A leaf consists of a petiole, a float (in small plants or those living in very open areas) a blade and possibly an isthmus (tenuous portion between the float and the blade). Floats are located in the petiole. They are round or pear-shaped and range from 2 to 4 cm in diameter. They are formed when the physiological availability of water to the plant is great (Rao, 1920); hence, in very dense stands of water hyacinths, floats are usually absent. Petiole length increases with increasing plant standing density (Tucker, 1981). At 5

kg/m^2(wb), petiole length was 22 cm at 20 kg $/m^2$ (wb), length was 43 and at 40 kg $/m^2$ (wb) length was 50 cm. Generally, the float type of leaves are disposed in a nearly horizonal position (15 to 45° from horizontal) whereas the equitant leaves (e.g. leaves whose bases overlap within or above them) approach verticality (75° from the horizontal) (Penfound and Earle, 1948). In dense stands, water hyacinths' leaves grow upright rather than horizontally over the water surface (Reddy, 1988).

Stolons originate from a rhizome and produce new offshoots of hyacinths at their distal ends. Stolons can be relatively short and vertical in dense mats but long and horizontal in open conditions. They are 1 to 2.5 cm in diameter and 4 to 22 cm long in open stands or 5 to 8 cm long in close stands (Penfound and Earle, 1948 and Zamora et al., 1982).

Internal structures of various organs of the aerial part of a plant are similar to each other (Zamora et al., 1982), and they can be classified into three groups: parenchymatous cells, support and conduction cells, and air spaces. Ninety-five percent of the biomass of a plant is parenchymatous or consists of unspecialized cells that usually have well-defined central vacuoles, and they are used typically for storage of protein, starch grains, oil, etc., or as chlorenchyma cells in the blade.

Collateral vascular bundles, a collection of phloem and xylem cells, are scattered throughout the aerial part of a plant. Phloem functions in conduction of food, and xylem functions in conduction of water and minerals and to support. Besides vascular bundles, fiber and tracheids, which are types of xylem providing mechanical support

are commonly found in a plant. Interconnected fibers are abundant in blades, roots and petioles, but rare in stolons and rhizomes, while tracheids can be located throughout an entire plant. The fibers are 1.5 to 3 mm long by 2 to 10 µm in diameter, whereas tracheids are elongated and helical in shape and can be stretched far before they break.

Air spaces allowing water hyacinths to float are located in abundant intercellular spaces: air chambers and parenchyma cells. Air chambers or lacunae are particularly characteristic to parenchyma tissue, and they appear as narrow passages where cells seem to have been pulled apart at the corners by the continuous growth of the epidermis. The air chambers formed permits diffusion of gases and equalized pressure. The cross portions of the air chambers, known as diaphragms, prevent flooding because these structures are perforated with minute openings specific only for the passage of gases. The system of lacunae is continuous from leaves to roots.

Chemical Composition.

Basically, the water hyacinth consists of water. Penfound and Earle (1948) and Knipling et al. (1971) determined that 93 to 95% of the fresh content of roots, 95.1% of rhizomes, 96.7% of stolons, 93.8% of floats, and 87 to 89.3% of blades is water.

Depending on the standing density of plants, 50 to 65% of the dry weight of a plant is fiber (cellulose, hemicellulose and lignin), around 40% is carbon, and 1.3 to 3% is nitrogen, (Debusk and Dierber, 1984).

Density and Buoyancy

The densities of various parts of plants were determined by the volume weight method by Penfound and Earle (1948). He found that the specific weight of a root was 0.782, of a rhizome, 0.805; of a stolon, 0.818; of a float, 0.130 and of a blade, 0.741.

Penfound and Earle (1948) also observed the loading capacity defined as the weight required to submerge a mat of plants, of a 1.5 m^2 mat of plants to be 177 to 430 N/m^2 (Pa). The latter corresponded to a population density of 200 plants/m^2.

Materials and Methods

Extensive literature exists concerning growth rates, morphology and chemical composition of water hyacinths. Insufficient information existed to establish criteria that could be used to physically distinguish different types of mats. This section presents the procedures that were performed to determine characteristics that physically defined water hyacinth mats.

Sample Size and Plant Characterization

Total plant length, aerial length, root length, largest leaf mass, plant leaf number, plant mass and blade mass were recorded as plant characterization.

The sample size of plants was chosen by time restraints and calculations based on sample variance, confidence interval and confidence level (Steel and Torrie, 1960). Choice of an adequate sample size to determine various physical characteristics of a mat was complicated, because each type of measurement had associated to it a different variance. In other words, sampling was from a bivariate distribution.

For example, calculations showed that within mats, plant mass was much more variable than plant length. Water hyacinths primarily reproduce through stolons; hence, plants of many sizes are expected in a given mat. Indeed, a sample standard deviation of plant mass calculated from a sample size of seven was over half of the average plant mass. Calculations based on this standard deviation indicated that a sample of 400 plants would be needed for a sample mean of plant mass to fall within 5 gm of the population mean with confidence 0.95. On the other hand, calculations based on an observed sample standard deviation of plant length showed that only 15 to 20 plants would be needed to obtain a population plant length within 5% of the true mean length and with 0.95 confidence. To obtain a population plant length within 10%, a sample of 5 to 10 plants would be needed.

In this study, except when otherwise noted, seven plants were characterized for size and component description per mat or aggregation. Seven plants permitted an accurate approximation for mean plant length, and the time to fully characterize a mat was permissible.

Plant Mass Distribution and Rhizome Length

The best least square relation to predict rhizome length from other plant characteristics was sought, and a classification of plant size based on mass was constructed to compare plant size histograms of different population groups.

Plants from the University of Florida Swine Research Unit, Biven's Arm, Lake Alice, and IFAS Zellwood, FL Field Laboratory were characterized according to the general procedure described in the

previous section except that more than ten plants were sampled (see results for exact numbers) and rhizomes were measured. Mats from these locations were sampled to obtain data that represents different plant sizes and conditions. The plants from the two lakes and from Zeliwood had long roots. The plants from Bivan s Arm were very big. Swine unit cultures were harvested periodically, and they had short roots.

The classification of plant size within mats was attempted by this method: first, sample populations of plants were measured to determine if the mass data was distributed normally (i.e. skewness was calculated). Once this was ascertained, the mass values were attached to plant size classes and their frequency noted. A histogram for each sample population of water hyacinths was plotted using the classes. Skewness was calculated from each frequency table to check if the distribution of the size classes within each mats was normal.

Connectivity, Buoyancy, and Areal Densities

After a physical analysis of water hyacinth mats, it was observed that mats could differ by average size of plants, standing density, mat buoyancy and connectivity. Except for connectivity, there were established methods to measure all of the mentioned characteristics, therefore, a method to measure connectivity was devised. Connectivity is a measure of the degree of entanglement through petioles and stolons. Zero connectivity is expected in mats where plants are not touching each other; and the plants are not connected by stolons. The principle of the devised connectivity test is that as connectivity increases, more weight/unit mat area is required to submerge a mat

Connectivity, buoyancy, and standing density were measured using the following equipment: a 0.74 m^2 rigid, mesh steel frame, weights and a scale. Measurements were performed as follows:

A mesh steel frame was placed on top of undisturbed mats. Weights were placed on the frame until it was just under the water. The weights were removed, frame and mat were cut away from the surrounding plants, and weights were added again. After each test, plants were characterized, and all the plants within the frame were weighed and counted. The test was repeated several times at the Swine unit on different types of plant mats and twice at Zellwood. Mat buoyancy was calculated as pressure to submerge the non-connected plants over the area of the frame (Pa) and connectivity as the difference between the pressures to submerge the connected and non-connected plants (Pa). Some mats had similar buoyancy values but different connectivities. To ascertain easily the affect of connectivity on mat stability, the ratio of connectivity to mat buoyancy were calculated for every mat tested, and this ratio was termed connectivity ratio (%). The best least square relations to predict population density and buoyancy from other mat characteristics were sought.

Results and Discussion

Plant Mass Distribution Histograms

All but one of plant mass data sets for the mats sampled had normal distributions; however, mean values were different. Skewness values ranged from -0.1 ± 0.6 to -0.3 ± 0.8 for the normal populations. Skewness was 1.5 ± 0.6 for the unsymmetrical distribution. A skewness value of zero signifies a normal population

Its standard deviation is given by the square root of six divided by the number of samples (Press et al., 1986).

Plant size was represented by six classes and various subclasses (Table 3.0); this classification system may have to be expanded by the addition of other subclasses to fit other population groups not sampled. Class 0 represents plants that weigh less than 0.1 kg. This class was subdivided into subclasses, because the largest and smallest plants in a given population fell within only two adjoining classes (e.g. the smallest plant fell into class 0 and the largest in 1). Class 5 represents large plants that weigh over 0.7 kg. The class structure follows a linear increase in mass until class 3. Classes 3 through 5 allow for greater mass differences because larger and older plants are structurally different from younger and smaller plants. Larger plants usually have more leaves and fewer stolons, and they have part of their mass in decaying leaves that eventually slough off.

Table 3.0. Plant mass classes

Class	Subclass	Plant mass kg
0	2	0.02-0.04
	4	0.04-0.06
	6	0.06-0.08
	8	0.08-0.10
1	1.0	0.10-0.13
	1.3	0.13-0.17
	1.7	0.17-0.20
2		0.20-0.30
3		0.30-.50
4		0.50-.70
5		> 0.70

Histograms constructed with these classes were normally distributed (Figures 3.1 - 3.3), and these mass distributions came from well-established population groups. Mass averages varied according to age of culture or habitat. After the data from the one unsymmetrical group (Figure 3.4) was studied, it was determined that the population could be represented by more than one group of plants, one dominated by class 0 plants and the others by higher classes (Figure 3.5). This group of plants was not well established because their population was controlled by regular harvests. The histograms illustrate that water hyacinth size could greatly differ from one location to another and even within the same location if the population is still not well established.

Rhizome Length

Data on rhizome length from all locations were aggregated and graphed together. Rhizome length is linearly correlated to plant weight (Figure 3.6). Length varied from 1 to 21 centimeters. Two least square equations that relate rhizome length to plant mass were evident: one for plants that showed considerable weevil damage or mass concentrated in the rhizomes and one for healthy plants with ample foliage.

Areal Density

Biomass density in this study varied from 8 to 20 kg/m^2 (wh) and population density varied from 40 to 300 plants/m^2. However, an apparent relationship exits between the two types of density (Figure 3.7). One estimate of population density is the quotient of the biomass density (kg/m^2) of a given aggregation by its average plant mass (average of 7 plants). This simple relation functions well for

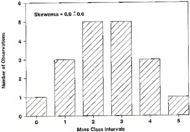

Figure 3 1 Distribution of plant mass in a well-established population. Plants were located in Lake Alice, and they averaged 0.035 kg.

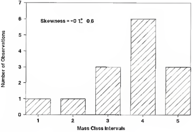

Figure 3.2 Distribution of plant mass in a well-established population. The plants were located in Bivan's Arm, and they averaged 0.6 kg.

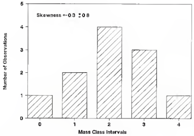

Figure 3.3 Distribution of plant mass in a well-established population. The plants were located in a pond that received agricultural waters. The plants averaged 0.25 kg.

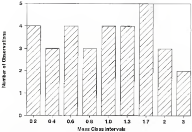

Figure 3 4 Mass distribution in a population that was not well established The culture had been harvested periodically Plants were from the Swine Unit.

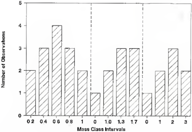

Figure 3.5 Mass data used in Figure 3.4 were redistributed to show that a population that is not well established could consist of many mass groups

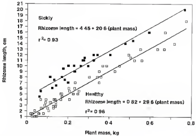

Figure 3.6 Rhizome length is correlated to plant mass Mass of sickly plants is concentrated in rhizomes.

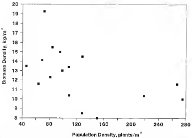

Figure 3 7 No apparent relation exists between areal mass and population density of water hyacinths.

population densities less than 100 plants/m^2, but it is very unreliable for aggregations of small plants or large populations (Figure 3.8). Small plants usually indicate a population that is not well established, in which case a reliable value for plant mass can be difficult to obtain (Figure 3.4). A more accurate prediction of plant number was established (Figure 3.9). The relation was developed from Tucker's (1981) observations that biomass density increased with petiole length. The least square relation is a nonlinear relation involving the logarithm of average plant height. Biomass density and average plant length are the independent variables. Both of these relations were established for populations with short roots, hence, they should not be used for long-rooted plant systems.

Connectivity and Buoyancy.

Mat buoyancy in this study varied from 20 to 240 Pa and connectivity from 20 to 180 Pa (Table 3.1). Penfound and Earle (1948), on the other hand, found that loading capacity varied from 177 to 430 Pa. The larger value, 430, probably represented data from an extremely compact aggregation.

Mat buoyancy did not correlate well with standing mass or population density, although buoyancy appeared to increase somewhat with areal mass density. The relation between mat buoyancy and areal mass density became evident when the data were parameterized by the ratio of connectivity to mat buoyancy (Figure 3.10). The least square relations are presented in Table 3.2. The highest buoyancy at any given areal mass density occurred when connectivity ratios were less than 0.4, and the lowest mat buoyancy occurred when the connectivity

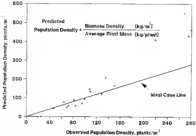

Figure 3.8 Method to estimate population density effective for low areal plant densities using mass average of seven plants. The straigth line represents the theoretical case of perfect correlation between predicted and actual responses. Region of discrepancy is for high densities

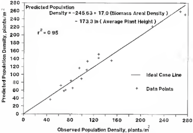

Figure 3.0 This equation predicts accurage values for population density. Population density depends on areal density and plant length. The straight line represents the theoretical case of perfect correlation between predicted and actual responses.

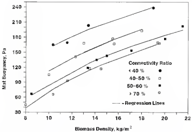

Figure 3.10 Mat buoyancy is dependent on areal mass density, and type and condition of plants. Connectivity ratio reflects type and condition of plants in a mat

Table 3 1 Values of mat buoyancy connectivity and connectivity ratio

Mat buoyancy	Connectivity	Connectivity ratio	Areal density	Average plant length
Pa	Pa	%	kg/m^2	cm
165 0	22 8	14 0	10 4	16 6
169 0	47 7	28 0	11 8	17 0
203 0	62 8	31 0	13 4	47 0
238 0	90 6	38 0	18 0	27 1
105 0	42 0	40 0	10 0	15 2
140 0	56 4	40 0	12 3	50 0
167 0	78 5	46 0	15 6	53 8
166 0	70 6	42 0	13 0	52 0
177 0	74 9	42 0	15 5	76 0
193 0	76 2	40 0	18 0	18 5
85 7	38 2	67 0	8 5	24 6
118 0	59 0	50 0	13 5	74 1
135 0	76 1	56 0	14 0	69 4
143 0	71 5	50 0	15 0	54 0
133 0	71 8	54 0	17 0	46 7
177 0	95 6	54 0	20 0	42 9
202 0	119 2	59 0	21 5	52 7
44 8	39 4	88 0	8 0	24 3
66 0	50 8	77 0	10 4	31 0
93 0	68 8	74 0	11 8	50 0
119 0	102 9	86 5	13 4	21 0
117 0	89 5	76 5	14 6	42 0
170 0	119 0	70 0	18 4	36 0
102 0	78 5	77 0	16 7	57 9
92 2	181 6	197 0	22 7	59 0

NOTE The last two entries represent data from long-rooted plants

ratios were greater than 0.7. Mat buoyancy is affected by connectivity ratio because the ratio reflects the type and condition of plants comprising a mat. High connectivity ratio indicates the plants are supported by petiole entanglement or are interconnected by stolons, while a small ratio indicates many petioles are floated and individual plants are supporting themselves. Petioles with floats and plants of low connectivity are common when a culture is periodically harvested, because open conditions lead to float formation in plants of any size (Rea 1980). Low connectivity results when plants are separated. Floats increase mat buoyancy, because the specific gravity of a float is 0.136 or one-fifth the density of a regular petiole.

Table 3.2. Relation between mat buoyancy (MB) and standing biomass density (BD).

Equation	Connectivity ratio	r^2
MB = -262.0 + 144.5 ln(BD)	> 70	0.98
MB = -235.8 + 139.2 ln(BD)	50-60	0.98
MB = -212.3 + 141.2 ln(BD)	40-50	0.90
MB = -135.0 + 127.4 ln(BD)	< 40	0.86

Two values for buoyancy were collected for long-rooted plants, and they were smaller than those expected for short-rooted plants with similar connectivity and standing densities. This is expected because

long-rooted plants have around 25% more biomass underneath the water as compared to shorter-rooted systems.

Summary.

Water hyacinths consist primarily of water, and although complex structurally, they can be defined by leaves, rhizomes, roots and stolons. Floatless petioles help support the plant under dense conditions by entanglement with leaves from other mats. Rhizome length is correlated to plant mass, and root length to nutrient availability.

Established populations of water hyacinth have normally distributed plant mass, while aggregations of small plants or plants subjected to regular harvests can consist of many types of plant groups.

Population density is correlated with plant length and standing biomass density.

Connectivity and mat buoyancy are independent properties that define the mechanics of the vertical stability of mats and plants

CHAPTER IV
VISCOUS AND ELASTIC PROPERTIES

A system is a collection of interacting elements for which there are cause-and-effect relationships among the variables. A water hyacinth system can be subjected to friction and elastic forces resulting from interactions of plants with each other, external driving forces of wind or towing devices and drag from the interaction of plants with water. Therefore, probable system elements are related to body forces (inertial and gravitational) and surface forces (pressure and shear). To represent the elastic and frictional forces in form of system elements, constitutive equations are required. They depend only on the characteristics of the physical material that comprises an element and on its geometry and they describe basic relationships between two variables (e.g. Hooke's law in solids and Newtons viscosity law in fluids).

Hydrodynamic Drag Forces

The purpose of this section is to develop the constitutive relationships between drag and towing velocity as a function of size of an aggregation of water hyacinths and plant size and shape.

Review of Literature.

Roots, rhizomes and lower petioles of water hyacinths are submerged in water. When they are placed in flow, they are subjected to drag. Drag is composed of two components: friction drag resulting from tangential stresses caused by friction of the fluid against the interface, and pressure or form drag, resulting from pressure forces exerted by the fluid normal to the surface of the body. The latter is predominant at high Reynolds numbers. Drag on a body can be determined analytically for simple shapes and flows and numerically for slightly more complicated geometries, but it is usually determined experimentally for bodies in turbulent flow. Customarily, the formula for overall drag is written in the following form

$$D_f = \frac{C_d\ A\ \rho\ V^2}{2}, \qquad (4.0)$$

where D_f is drag force, A is a the area of the body projected in the direction of flow, ρ is density of the fluid, C_d is a drag coefficient and V is the velocity of the fluid relative to the body which may move or be stationary.

A similar drag formula was initially proposed by Newton, but the original proportionality factor (instead of C_d) did not always coincide with experimental data. This problem was resolved when a function of Reynolds number was used to replaced the original proportionality factor (Prandtl and Tietjens, 1934). Reynolds number enabled calculation of drag in a Newtonian fluid on similar bodies which have the same orientation with respect to the free stream velocity. The relation between C_d and Reynolds number must be

determined for turbulent flow only experimentally. Furthermore, experiments proved that when the total drag on a body consists exclusively of pressure drag (i.e., for high Reynolds numbers), the drag coefficient is large and independent of Reynolds number. In the case of friction drag, the drag coefficient is a function of Reynolds number, and it is usually small in value.

Rhizomes are the principal projections into water; they are cylindrically shaped. Due to the shape of rhizomes, water hyacinths in flow can be modeled from flow analyses for a series of cylinders (e.g., in a heat exchanger). Also, information concerning the flow properties of water hyacinth can be ascertained from a review of studies of flow retardance by aquatic plants, which are assumed to represent roughness elements. These topics will be reviewed next.

Flow normal to a bank of cylinders. Since the shape of rhizomes can be assumed to be cylindrical, the following information on crossflow over a bank of cylinders is pertinent to the description of water hyacinth behavior. Grimison (1937) correlated shear stress, τ_s, to mass flow rate:

$$\tau_s = \frac{F\, p\, G^2}{g\, \rho} \tag{4.1}$$

where G equals mass flow, p is the number of major restrictions encountered by flow through a bank, and F is a friction factor which is a function of Reynolds number and the ratio of transverse to longitudinal spacings.

He found that friction coefficients for different arrangements of cylinders were functions of Reynolds number (based on cylinder

diameter), the number of major restrictions encountered in flow through the bank, and the ratio of transverse to longitudinal spacing. The number of major restrictions depended on the configuration of the cylinders: for in-line arrangements, p equaled the number of rows; for staggered arrangements, with minimum flow area in transverse intertube spaces, p equaled the number of rows, and for staggered arrangements with minimum flow area in diagonal intercylindrial spaces or openings between cylinders, p equaled the number of rows minus one. Generally, the friction factor was constant until Reynolds number exceeded 10,000. Above 10,000, the general characteristic curve for friction factor inclined downward.

Later, the equation for total head loss due to friction was refined to resemble the friction factor from a Moody diagram (Equation 4.4) (Kays and London, 1984 and McQuiston and Parker, 1982).

Total head loss (Kays and London, 1984) =

$$Y_s = F \frac{A}{A_c} \frac{V^2}{2g} \qquad (4.2)$$

where F is Moody friction factor, V is mean velocity, $\frac{A}{A_c} = \frac{4\ell}{R}$, A is total friction area, A_c is total flow cross sectional area, and ℓ is flow length. Both A and ℓ are measured from the leading edge of the first cylinder row to the trailing edge of the last row of cylinders, and R equals the hydraulic radius. Hydraulic radius for flow normal to cylinders is cylinder diameter.

Roughness elements and hydraulic resistance. Hydraulic resistance is often presented in an alternative form that was derived by dimensional analysis (Lamb, 1945).

$$D_f = \frac{\rho}{2} A \left(\frac{\nu}{V a}\right)^m V^2, \qquad (4.3)$$

where a is a characteristic length, ν is kinematic viscosity, V is average velocity of a cross section and m is an exponent obtained through experimentation. Reynolds number is defined by $\frac{V a}{\nu}$. For $m=0$, the formula that is often used in hydraulics for the case of turbulent flow through pipes is obtained. It is similar to Equation 4.0. Lamb (1945) suggested that the value of m appears to depend on the smoothness of a surface.

Without exception, studies of flow retardance by aquatic plants have assumed that plants in channel flow act as roughness elements. Basic ranges of flow regimes for roughness elements have been established on the basis of height and spacing of roughness elements (Schlichting, 1979). These are 1) the hydraulically smooth regime where the size of the roughness is so small that all protrusions are contained within the viscous sub-layer, 2) the transition regime where protrusions influence the viscous sub-layer, and the resistance compared with a smooth pipe is due mainly to form drag experienced by the protrusions in the turbulent boundary layer, and finally, 3) the completely rough regime where all protrusions extend outside the viscous sub-layer and the resistance is due mainly to form drag. These regimes are determined by the following criteria

a. Hydraulically smooth

$$\frac{k_s V_*}{\nu} \leq 5; \quad F = f(\text{Reynolds number})$$

b. Transition

$$5 \leq \frac{k_s V_*}{\nu} \leq 70, \quad F = f(\frac{k_s}{R}\ \text{Reynolds number})$$

c. Completely rough

$$\frac{k_s V_*}{\nu} \geq 70; \quad F = f(\frac{k_s}{R})$$

where k_s denotes the grain size in Nikuradse's sand roughness, V_* is the friction velocity defined by $\sqrt{\tau_o/\rho}$, R is the hydraulic radius, $\frac{k_s V_*}{\nu}$ is often referred to as the wall Reynolds number, and τ_o is shear stress at the wall. Friction factor (Darcy-Weisbach) is related to shear stress by $\sqrt{\tau_o/\rho} = \sqrt{F/8}\ V$. Furthermore k_s has been related experimentally to Manning's n (Stricker, 1929)

$$n = (1/26)\ k_{s(65)}^{1/6} \qquad (4.4)$$

with units $m^{1/3}s^{-1}$ and $k_{s(65)}$ is roughness in meters such that 65% of the material is of lesser size. The equation is valid for $4 < \frac{R}{k_s} < 4000$. Manning's n is a roughness coefficient; its value increases with increasing roughness.

In reference to flow over aquatic plants, Ree and Palmer (1949) demonstrated by experiments that the degree to which bottom channel vegetation retards water flow depends largely upon the degree to which vegetation is bent and flattened by the flow, which in turn, depends mainly upon physical characteristics of the vegetation, its manner of growth, and the velocity and depth of flow. The plants were different kinds of grasses and kudzu. More specifically, when flow was sufficiently deep and fast to bend over and submerge the channel

vegetation, a greater velocity resulted due to a greater slope of the energy grade line resulted in lower resistance to flow. Manning's n values for short and medium-height vegetation appeared to decrease to a nearly constant value of about 0.035 as depth of flow was increased to cover the plants. Values of n for different tall plant species varied widely for all depth of flows. In regard to population density for a specified flow depth, a dense cover of vegetation (300 plants/m^2) offered twice as much resistance to flow as a less dense cover (17 plants/m^2). The authors developed a graphical method for the determination of channel cross section. To do so, they plotted Mannings n values versus VR (velocity times hydraulic radius) because they perceived resistance to be a function of the degree of flattening of the vegetation, which is influenced by velocity and depth of flow. As a result, they found that until a given vegetative channel lining became well flattened, the value of VR indicated the degree of resistance the lining offered. However, when the vegetation was prone, or nearly so, and well submerged, n became practically constant and ceased to correlate with VR.

On the other hand, Kouwen and Unny (1973) determined two values for the local friction factor, one for erect and the other for prone regimes. They found that friction for the erect and waving regime was a function of a relative roughness factor, while for prone plant roughness, friction factor was a function of VR. The experimental results were in the form of graphs. This apparent discrepancy in the two investigations could relate to the amount the vegetation was submerged or to the depth of flow. Although, it appears that Kouwen and Unny were correct in their conclusion because 1) flow theory of

a fully rough regime in a channel predicts the drag coefficient to be independent of Reynolds number, so drag varies with V^2 and is independent of viscosity, and 2) erect vegetation is more likely to cause a fully rough flow regime because the roughness elements are bigger to provoke larger values for the wall Reynolds number.

Many investigators have found that Mannings n or friction coefficient increases with the amount of aquatic biomass present (Ree, 1949; Kouwen et al., 1969; Powell, 1978; Petryk and Bosmajian III, 1975; Shih and Rahi, 1982 and Stephens et al., 1963). Petryk and Bosmajian III (1975) defined density of aquatic vegetation by the vegetative area per unit length of channel per unit area of flow as expressed by the following equation

$$\text{Density of vegetation} = \frac{\Sigma A_i}{A\,\ell}$$

where A_i = projected cross sectional area of vegetation in the flow direction in a channel of length ℓ and cross area A.

The effect of plant density on flow retardance can be related to roughness spacings. Powell (1946) studied longitudinal spacing of strips in a channel. He found that the ratio of roughness spacing to roughness height was an important determinant of maximum relative roughness, and it was constant regardless of the value of the roughness width to height ratio. Sayre and Albertson (1961) studied both longitudinal and transverse roughness spacing, and he used dimensional analysis to develop the following spacing parameter.

$$\text{Spacing parameter} = \frac{hb}{x(x + b)} \qquad (4.5)$$

where x = longitudinal spacing of roughness baffle, h = roughness

height, b = roughness width and m = transverse spacing length. The flow was considered to be in the completely rough range. Data were analyzed in terms of Von Karman-Prandtl concepts of turbulent flow near a rough boundary, and the following equation was fitted to the data.

$$\frac{C}{\sqrt{g}} = 5.06 \log \frac{y_n}{h} + C_2$$

where C is the Chezy discharge coefficient = $R^{1/6}/n$, y_n is normal depth, C_2 is an experimental constant dependent on roughness spacing, h is height of roughness element, and g is acceleration of gravity. Similarly, using the equation for logarithmic velocity profile near a turbulent wall, Kouwen et al. (1969) obtained this equation for flow velocity in a vegetated channel:

$$\frac{V}{V_*} = C_1 + C_2 \ln \frac{A}{A_v}$$

where C_1 and C_2 vary with the vegetative density and the flexibility of the vegetation. A is the gross cross sectional area of the channel and A_v is the area of vegetative cross section.

In summary, the most relevant concepts discussed in this section for application to water hyacinths are:

a. Theory and experiments have shown that bigger plants and denser vegetation produce a larger drag coefficient.

b. Empirical relations for pressure drop across banks of cylinders in cross flow have shown that cylinder diameter and size of

the bank specifically, cylinder length, bank length and bank width, influence friction factors

c For Reynolds number (based on tube diameter) less than 10 000 the friction factor of a bank of cylinders in cross flow is independent of Reynolds number

d Transverse and longitudinal spacings of cylinders in cross flow and of roughness projections in flow affect drag coefficient

e Plants that are flatten in flow offer less resistance to flow than erect plants

f Experiments have proven that when vegetation is erect the drag coefficient is independent of Reynolds number, and it is dependent on a relative roughness parameter

Drag Model for Water Hyacinths.

In this section, an expression for drag valid for a rectangular aggregation of plants of any population density or spacing and frictional area in flow is developed in this section Neither numerical nor analytical solution appeared feasible for the problem of water hyacinths in steady flow due to the assumptions of 1) rhizomes and roots cause turbulence and 2) the mat deforms when moved Therefore, an analytical solution based on rigid, rough flat plate is not appropriate. Consequently a drag model was developed based on Newton's drag equation (Equation 4 0), and drag coefficients were obtained experimentally

To begin, a model for drag must be dimensionally correct. The drag equation, Equation 4 0 was used after it was modified by the incorporation of the number 2 into the drag coefficient

$$D_f = \rho \; A \; C_d \; V^2 \qquad (4.6)$$

where D_f equals the drag force (Newtons), ρ equals the density of water approximately equal to 1000 kg/m^3, A equals the projected area in flow (m^2), C_d equals a nondimensional drag coefficient and V is the towing velocity (m/s). Although Equation 4.6 implies C_d is a function of Reynolds number, evidence in the literature indicates that the drag coefficient for an erect, rigid projection like a rhizome of water hyacinth, is independent of Reynolds number. If indeed, C_d of water hyacinths is independent of Reynolds number, the towing velocity would enter the model only as V^2. To substantiate this, the Reynolds number was calculated. Diameters of rhizomes range from 0.01 to 0.03 m. The Reynolds number for water hyacinth based on a 0.01 m diameter and a towing velocity of 0.4 m/s is calculated below.

$$\text{Reynolds number} = \frac{\text{Diameter of Rhizome x Towing Velocity}}{\text{Kinematic Viscosity}}$$

$$= \frac{0.01 \times 0.4}{0.804 \times 10^{-6}} = 4975.0$$

However, for 0.03 m diameter, the Reynolds number is approximately 15,000. At 0.4 m/s, which was usually the observed upper limit of stable towing operation, medium and small rhizomes can be expected to have Reynolds numbers below the lower limit at which drag of cylinders in cross flow is dependent on Reynolds number.

To use the drag equation, the friction area must be defined. The total friction area was assumed to approximately equal the projected

area of a rhizome (A_r) multiplied by the total number of plants (N_p) in an aggregation or

$$A = N_p D_r L_r = N_p A_r \tag{4.7}$$

D_r equals the average diameter of the rhizomes and L_r, average length.

The shape of a water hyacinth mat also influences the drag coefficient since drag coefficients are only similar for geometrically similar bodies of the same orientation in relation to the free stream velocity. Therefore, a mat which is wider or has more plants along the flow direction will have a different drag coefficient than a narrower mat. The shape factor enters the cylinderical crossflow models as p (Equation 4.4) and nondimensionally as A/A_c (Equation 4.5). For a rectangular mat of water hyacinth, the simplest nondimensional shape factor is the ratio of the two dimensions, i.e. width, W, to length, L.

For this study the transverse and longitudinal spacings of water hyacinths within a mat was assumed uniform. As a result, the drag coefficient was considered to be a function of a shape factor and possibly, Reynolds number. Then the proposed drag model for water hyacinth becomes

$$D_f = \rho N_p D_r L_r C_d V^2 \tag{4.8}$$

where,

$$C_d = f\left[\frac{D_r V}{\nu}, \frac{W}{L}\right]$$

This proposed equation is valid for any rectangular aggregation of water hyacinth without the need for graphs or tables to determine C_d, provided, of course, that C_d is obtained experimentally.

Materials and Methods

This section presents the procedures that were used to 1) test the hypothesis that the drag coefficient of a water hyacinth mat is independent of Reynolds number and 2) determine the empirical relation of C_d to mat geometry.

Plant material

Aggregations of water hyacinths composed primarily of small, medium or large-sized plants were towed. Small plants averaged 25 cm in length; medium plants averaged 61 cm and large plants averaged 90 cm. Whenever the water was deep enough, a buoyancy test was performed on the mat before it was moved to the testing area. Water hyacinths were obtained from the University of Florida Swine Research Unit, Glen's Arm, and Lake Alice. The lakes are located near the University of Florida. After completion of each experiment, seven plants were measured for mass, rhizome length and diameter, largest petiole length, plant length and root length. Root length varied according to habitat and ranged from 2 to 24 cm. The presence of stolons and floats was noted.

Aggregations of plants from the Swine Unit were relocated to the testing area in this manner. First, a 2.44 by 1.22 m area of plants was isolated; then, a frame of wood and fence wire was positioned underneath the plants. Lifting the frame removed the plants from the water in their natural positions. Because the water was too deep at

the two lakes, the hyacinths were dragged to shore and hand positioned on the frame.

Towing experiments.

To measure the drag coefficient of water hyacinths, towing experiments were performed on different sizes of rectangular aggregations of water hyacinths. The tests were performed in the hydraulics lab., Civil Engineering Department, University of Florida. The following equipment were used: an adjustable force sensing, floating frame-like structure, a powered trolley, water velocity meters and instrumentation (Figure 4.0).

The floating structure consisted of two frames, an outer supporting structure of 38 x 38 x 1.5 mm square, steel tubing on two 168 mm PVC pontoons and an inner containment frame of 25 x 25 x 2.1 mm square, steel tubing. The inner frame weighed approximately 12 kg and was suspended from the outer frame by four restrained cantilever beams instrumented with temperature-compensated, bonded strain gage bridges. The elevation of the outer frame above the pontoons was incrementally adjusted so that the inner frame just cleared the water. Arrangement of the two frames assured that water hyacinths contained in the lower frame could not touch the upper frame. The inner frame was fitted with 6 mm rod tines projecting 338 mm below and 150 mm above the frame bar to prevent plants from climbing over or rolling under the frame, and, it was arranged to be sub-divided into 2.4 m long x 1.2 m wide, 1.8 m x 1.2 m, 1.2 m x 1.2 m, 1.2 m x 0.6 m, and 0.6 m x 1.2 m containment areas. The 0.6 m x 1.2 m containment area had tines placed all around

Figure 4.0 Towing equipment included a frame-like [illegible], force sensing devices, and a trolley

it because the plants escaped from the sides during preliminary experiments

The length of each cantilever beam was 0.30 m and the width and thickness were 5.08 and 0.32 cm respectivity. One 350 ohm strain gage was attached to each side of a cantilever beam; hence, two four gage bridge circuits, one for each end of the frame, were used to measure the forces against the beams. The force measuring system was calibrated by using a spring scale and by recording the corresponding voltage (Figure 4.1).

Towing velocity was recorded by two methods. Propeller type velocity meters (A. Ott Kempten current meters) attached to the trolley, were used in the initial tests. After the meters failed to function properly, distances along the towing path were marked off and time to travel a distance was recorded through the aid of video equipment.

The force and velocity signals from the two rigs were recorded by a Campbell Scientific CR7 data logger with observations recorded every second.

Before some of the tests, a grid of thin nylon twine was placed over the set of plants for subsequent observation of plant movement in relation to each other. The tests were videotaped. Some underwater observations were visually recorded through a glass window in the side of the channel.

A typical experiment proceeded as follows. Plants were placed into the containment frame. The frame was pulled by a trolley through a 2.4 m wide channel with the water depth kept at 0.51 m. Plants were

Figure 4.1 Strain gages were attached to cantilever beams which were suspended from the upper frame and attached to the lower frame. The lower frame contained plants. Towing velocity was measured by a current meter

towed at a constant speed for a distance of approximately 11 m. Towing speed was increased from 0.1 to 0.6 m/s until the plants started to roll under the containment structure. When this happened, the test was ended and the sample was subdivided. Some of the plants were removed to obtain weather mat size. Removed plants were drained and weighed to determine the quantity of biomass in the sample. Towing tests were repeated on sequentially smaller mats until all mat sizes were tested.

Analysis of data.

Force and velocity data for each test were regressed according to the equation

$$D_f = C_e V^2 \qquad (4.9)$$

where D_f equals total drag force in Newtons, C_e is a constant of proportionality equal to the product of $(\rho N_p D_r L_r C_d)$ from Equation 4.8 and V equals towing velocity. Drag force was determined to be the force on the cantilever beams after the plants had stopped accelerating and the forces due to the acceleration stage of the test had diminished to a slight fluctuation. The parts of the towing tests were labelled the unsteady and steady stages (Figures 4.2 and 4.3).

The data were analyzed for error. Random or experimental error can be quantified when its distribution approaches a normal distribution (Herschy, 1976). The principal source of experimental error was the data logger. Drift of the set point of the data logger was ± 0.083 mv, which translates into an error of ± 0.9 N. Skewness of the force data during the steady state conditions of a towing test

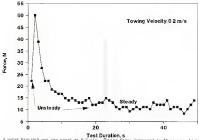

Figure 4.2 A water hyacinth mat was towed at 0.2 m/s. Towing force decreased to fluctuate slightly in the steady portion of the curve.

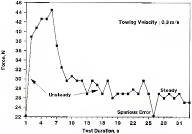

Figure 4.3 A water hyacinth mat was accelerated slowly to a final velocity of 0.3 m/s. Spurious errors were found in test data. Steady and unsteady portions of the curve are marked.

was calculated for two runs (towing velocities, 0.2 m/s and 0.3 m/s) and the values were -0.28± .18 and 0.35 ± .39. If skewness is zero the distribution is normal, accordingly, the force distribution can be considered to be normal. A histogram of the drag force distribution is shown in Figure 4.4. The dispersion of drag force about the time average was measured in standard deviation since the distribution was normal. Standard deviation of drag force, D_f, was calculated using data from the two tests while standard errors of D_f (Equation 4.10), drag force calculated from the regression model, and of the coefficient C (Equation 4.11) were computed for every test. Since the International Standards Organization has recommended that the probability level used should be at the 95 percent level (Herschy, 1978), error was reported using the corresponding t statistic multiplying either the standard error or deviation.

Standard Error of Estimate, S_e (Herschy, 1978),

$$S_e = \left[\frac{\Sigma (d^2)}{N - 1} \right]^{\frac{1}{2}} \tag{4.10}$$

where d is the deviation of the actual value from the computed value taken from the curve of relation or $D_f - D_f'$ and N is sample size.

Standard Error of the Coefficient (Herschy, 1978) is,

$$S_c = \frac{(N - 1)\, S_e^2}{(N - 1)\, \Sigma\ V^4 - (\Sigma V^2)^2} \tag{4.11}$$

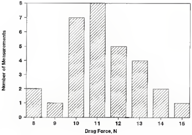

Figure 4.4 Histogram of drag data obtained from the steady portion of a towing test. Towing velocity was 0.2 m/s. Skewness indicated a normal distribution.

Spurious errors were discarded (Figure 4.3) when data lay more than q standard deviations from the sample mean. The value of q depends upon the sample population size (Benedict, 1985). For example, for a population of ten, q equals two.

Systematic error in the flow tests could be related to the design of the test frame. Tines retained plants within the test frame. The resistance to flow that was considered small, because the diameter and number of tines were small relative to those of the rhizomes. Moreover, the drag of tines on all but the 1.22 m long by 0.6 m wide test frame, which had more tines, was measured as 1.3 N at a towing velocity of 0.1 m/s and 3.6 N at 0.5 m/s. The drag on the smaller frame was nearly 30 % higher than the drag on other frames. Tines are required in any towing system, so their exclusion from the experiments was not deemed necessary. Also, force measurements could be susceptible to systemic error if the calibration of the strain gages was inaccurate. The gages were calibrated twice using different input voltages, spring scales and ranges of force, and the calibration factors remained the same. Finally, another source of systematic error is the number of significant digits the data logger uses to store force readings. Too few and very small forces would not be recorded accurately by the data logger.

Results and Discussion.

Experimental observations.

At the beginning of a towing test, plants tended to bunch together, causing the length of the mat to decrease. Analysis of the movement of grid lines on top of the hyacinths demonstrated mechanisms of compaction. When a test began, the grid lines at the leading edge

of the mat remained stationary those at the rear moved Once the whole mat reached constant speed the grid lines were equally spaced again but closer due to compaction of the mat

Compaction increased with towing velocity until "roll under". "Roll under" occurred at a velocity exceeding 0 45 m/s At that point, the plants on the leading edge started to roll forward under the water Once under water, the plants tended to flatten out underneath the other plants moving on the surface In this way the plants on the surface passed over submerged plants and, in turn, rolled under when they were positioned at the leading edge (Figures 4 5 -4 7) At "roll-under", the force on the cantilevers greatly increased, and the portion of the force - velocity graph pertaining to "steady" was absent (Figures 4 8 and 4 9)

Some towing tests were repeated in an attempt to duplicate the results Data from repeated tests fell on the model line (Figure 4 9); hence, the tests could be duplicated under similar conditions

When plants are stationary, their roots hang downward in the water, yet, they are very flexible Underwater observations showed the roots to be completely prone at a towing velocity of 0 17 m/s and waving back and forth at lower speeds Once the roots were prone the component of drag was due to rhizomes.

Results of regression analysis

A model fits experimental data provided the standard deviation of the dependent variable falls in the range of the computed standard error of the predicted value. To determine the efficacy of the proposed model, time average values of the drag force were plotted against the square of the towing velocity for two sample tests The

Figure 4.5 When mats were towed, they compacted. Amount of compaction increased with towing velocity. At 0.1 m/s, compaction is slight.

Figure 4.6 The mat was towed at 0.3 m/s, and it compacted approximately 30 cm.

Figure 4.7 The mat was moving at 0.4 m/s, and it compacted approximately 60 cm

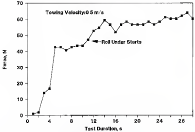

Figure 4.8 At "roll under", plants on the leading edge started to roll forward under the water. Towing force increased, and the portion of the force - velocity graph pertaining to "steady" was absent "Roll under" occurred at velocities exceeding 0 45 m/s.

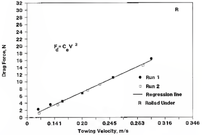

Figure 4.9 Drag tests can be duplicated under similar conditions up to the point that the mat starts to "roll under"

regression equation (Equation 4 9), the corresponding values of standard deviation (shown as SD), and error (shown as SE) were plotted (Figures 4 10 and 4 11). For the two tests analysed but excluding data for the largest towing velocity, the ranges of the standard deviations fell in the range of the standard error (95 confidence level). The fact that the ranges of the standard deviations of D_f at 'roll under ' velocity did not fall between the ranges of its standard error shows that the flow behavior of the water hyacinth changes near "roll-under".

Values of proportionality factor, C_e ,(Equation 4 9) were computed and errors are expressed to two significant figures (Table 4 0). In two tests, percent relative error was greater than fifteen, whenever the number of data points was less than five. Indeed, data sample size was not constant because some samples reached "roll-under" very quickly. In these cases, few data points were obtained. Morever 82 percent of the C_e values had less than ten percent relative error. Error was not consistent in each experiment nor between experiments. Values of the coefficient, also, appeared to vary according to physical variations in the mat and individual plant structure.

Drag Coefficient

Provided that Equations 4 8 and 4 9 accurately describe drag for any choice of plant and mat size and that C_d is not a function of Reynolds number, experimental drag coefficient should be nearly given by

$$C_d = \frac{C_e}{\rho \quad N_p \; A_T} \qquad (4\ 15)$$

where $C_d = f\left[\frac{W}{L}\right]$

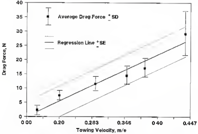

Figure 4.10 Error bounds about line of regression and drag. Mat area was 1.22 m x 1.22 m.

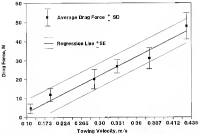

Figure 4.11 Error bounds about line of regression and drag. Mat area was 2.44 m long x 1.22 m wide.

Table 4.0 Coefficients for empirical equations that relate drag force to velocity data.

$$D_f = C_e V^2$$

$C_e \pm t\ S_e$		Number of data points	Sample size (LxW)	Density kg/m^2	Plant origin
Experiment 1					
242.0	12.0	7	2.44 m x 1.22 m	16.2	swine unit
206.0	26.0	7	1.22 x 1.22	15.2	"
190.0	52.0	3	0.61 x 1.22	17.0	"
102.7	6.90	8	1.22 x 0.61	17.0	"
Experiment 2					
206.0	19.0	6	2.44 m x 1.22 m	14.7	swine unit
262.0	35.0	6	1.22 x 1.22	20.3	"
146.0	11.0	7	0.61 x 1.22	23.1	"
76.0	15.0	4	1.22 x 0.61	23.1	"
Experiment 3					
236.4	8.70	11	2.44 m x 1.22 m	16.9	swine unit
260.5	6.90	7	1.22 x 1.22	19.0	"
156.2	8.70	7	0.61 x 1.22	21.3	"
67.6	2.40	11	1.22 x 0.61	21.3	"
Experiment 4					
equipment failure			2.44 m x 1.22 m		swine unit
263.0	17.0	7	1.22 x 1.22	13.6	"
189.0	23.0	6	0.61 x 1.22	11.6	"
65.9	8.0	6	1.22 x 0.61	11.6	"
Experiment 5					
109.2	6.70	11	2.44 m x 1.22 m	12.8	swine unit
82.7	6.10	6	1.22 x 1.22	12.4	"
116.2	8.70	6	0.61 x 1.22	15.8	"
41.0	4.30	5	1.22 x 0.61	15.8	"
Experiment 6					
196.0	14.0	12	2.44 m x 1.22 m	17.5	Given s Arm
188.0	16.0	6	1.83 x 1.22	17.3	"
156.0	10.0	9	1.22 x 1.22	16.9	"
151.4	13.0	7	0.61 x 1.22	14.9	"
64.4	5.30	11	1.22 x 0.61	14.9	"
Experiment 7					
245.0	24.0	6	2.44 m x 1.22 m	14.7	Lake Alice
162.0	12.0	6	1.83 x 1.22	14.4	"
188.3	8.80	6	1.22 x 1.22	11.6	"
136.0	19.0	6	0.61 x 1.22	12.6	

The values of C_d obtained by this expression from C_e are tabulated in Table 4.1 along with values of the shape factor and other variables. Variables N_p and L_r were calculated from expressions developed empirically in Chapter 3. Rhizome diameter is difficult to measure due to the presence of roots, but, since they have been known to vary little within a population or by as little as 0.5 cm, the following classification scheme was used: short plants have 1 cm diameters, medium plants, 2, and tall plants, 3 cm.

To assess the accuracy of the experimental drag coefficient experimental error of Equation 4.15 was calculated by the following equation (4.16) (Herschy, 1978).

$$E_{C_d} = \pm\left[E_C^2 + E_\rho^2 + E_{N_p}^2 + E_{D_r}^2 + E_{L_r}^2 \right]^{\frac{1}{2}} \tag{4.16}$$

where E_i denotes the percent error in the drag coefficient contributed by the i-th parameter. The error for each empirical value of C_e is shown in Table 4.0, and its average is approximately 10 %. Density of the water, ρ, could vary with the quality of water (dirty or clean) and temperature, but that error was assumed to be within 0.6 percent. The errors due to the estimation of N_p and L_r were assumed to be 10% and 3% respectively since that is approximately the error introduced by the empirical expressions of Chapter 3. The error due to D_r was estimated to be 3%. After substitution of these values of percent error into the error equation, the percent experimental error for the drag coefficients was 15%.

Table 4.1 Drag coefficient for different mat geometries and other mat characteristics

$$C_d = \frac{C_e}{\rho\, N_p\, A_r}$$

		Total number of plants	Width to length ratio	Flow area	Remarks on C_d
C_e	C_d	N_p	$\frac{W}{L}$	A_r	
Experiment 1					
242.0	0.73	518	0.5	8.4E-4	
206.0	1.33	242	1.0		
102.7	1.18	136	0.5		high
Experiment 2					
206.0	0.61	338	0.5	1.0E-3	
262.0	1.12	234	1.0		
146.0	1.10	133	2.0		low
78.0	0.59	133	0.5		
Experiment 3					
236.4	0.69	378	0.5	9.0E-4	
260.6	1.36	212	1.0		
156.2	1.46	119	2.0		low
67.6	0.63	119	0.5		
Experiment 4					
263.0	2.23	147	1.0	8.0E-4	high
189.0	2.63	90	2.0		
65.9	0.91	90	0.5		
Experiment 5					
109.2	0.74	613	0.5	2.4E-4	
82.7	1.15	300	1.0		
118.2	2.65	186	2.0		
41.0	0.92	186	0.5		high
Experiment 6					
196.0	0.66	74	0.5	4.0E-3	
186.0	0.87	54	0.67		
156.0	1.30	16	1.0		
151.4	2.37	16	2.0		
64.4	1.00	19	0.5		high
Experiment 7					
245.0	0.72	137	0.5	2.6E-03	
182.0	0.73	100	0.67		
188.3	1.02	74	1.0		
136.0	2.76	29	2.0		

The functional relation between C_d and shape factor W/L was ascertained. A regression equation relating C_d to W/L was determined to be nonlinear (Figure 4.12), and it is written below.

$$C_d = 0.4436 \exp(0.506 \frac{W}{L}) \qquad (4.18)$$

Not all values of C_d were used in the formulation of this relation because they were deemed to be outside of 95 percent confidence intervals. Confidence intervals of C_d were established for every shape factor $\frac{W}{L}$. The outliers were basically from two groups of mat sizes: four outliers originated from an area of 1.22 m long x 0.6 m wide, and two outliers from an area 0.6 m by 1.22 m. The former values were results of systematic error. They were related to tests resulting in the lowest drag values. As was mentioned before, these low forces may have been recorded improperly by the data logger. The offset value of the data logger added to the value of the real force. Two attempts were made to correct this problem. One method, which resulted in reasonable values of C_d (Experiments 2 and 3), was to amplify the input signal from the stain gages positioned on the cantilever beams. The second method, which involved supplying a higher voltage to the strain gages, was unsuccessful.

On the other hand, the two outliers from the other sample size could not be explained until after videotapes of the experiments were viewed. The plants were seen bending in the flow. The bending motion favored friction drag over pressure drag, therefore the drag coefficients were lower than expected (Schlichting, 1979).

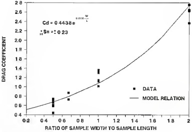

Figure 4.12 Drag coefficient of a water hyacinth mat is a function of mat geometry

The regression equation relating C_d to W/L was analyzed for experimental and dispersion errors. Dispersion of the data around the regression curve is given by tS_e where t is the t statistic (95 confidence level) and S_e is the standard error due to the regression. If the regression equation is valid, the confidence intervals of C_d for every shape factor $\frac{W}{L}$ should fall within the range of C_d given by the standard error of the regression. This was true except for W/L equal 2 (Figure 4.13). However, the discrepancy is negligible.

Summary

-Hydrodynamic drag coefficient of water hyacinths is independent of Reynolds number but dependent on the shape of a mat.

-The water hyacinth drag equation was based on Newton's drag formula, and it included the drag coefficient, projected area and number of rhizomes and the square of velocity.

Elastic Characteristics

Elastic deformation of water hyacinths occurs when an external force applied on a mat compresses plants against each other. Parts of the plants in contact during compression have been observed to be the rhizomes. The objective of this section is to determine experimentally the elastic modulus and Poisson's ratio of the rhizome.

Literature Review

Anatomical study of the rhizome reveals that it is a composite material of two or more components having various, usually contrasting physical and mechanical properties. Water hyacinth rhizomes, like other natural composites such as stalks of plants or bones of animals,

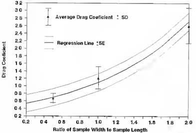

Figure 4 13 Error bounds about line of regression and drag coefficient

have ordered structure (Tarnapolskii and Kincle, 1981). Macro-structurally, the rhizome consists of four regions: outer region covered with profusely-branched roots of 0.4 to 1.5 mm diameter, epidermis, cortical region and stele. Rhizomes vary in length from approximately 1 to 20 cm and in diameter from approximately one to three centimeters.

Elastic properties are assumed to vary principally in the radial direction because of the symmetrical shape and radically varying structure of rhizomes. The elastic properties of a corn cob are similarly characterized and have been extensively studied (Anazodo, 1983; Anazodo and Chikwendu, 1983; and Chikwendu and Anazodo, 1984). The methods and equations these investigators used were adopted in this work to determine the elastic response of water hyacinths to contact of their cylindrical rhizomes.

Equations for the determination of elastic modulus E and Poisson's ratio ψ of rhizomes under quasi-static radial compression between two steel flat plates using a large deformation approximation, are (Chikwendu and Anazodo, 1984)

$$E = \frac{2\,P(1-\psi^2)\,(2/Y^4 - 5/6 + 67\,Y^2/288 - 475\,Y^4/24192)}{r\,(1 - Y^2/8 + Y^4/192)} \quad (4.19)$$

where P is the known experimentally applied force per unit length of the cylinder. Poisson's ratio ψ is calculated

$$\psi = \frac{(v/w)\lambda - 1 + \pi/4 + \eta_2(5(v/w) - 0.5) - (\eta_4/24)(7(v/w)/60 + 1)}{(v/w)\lambda - 1 + \pi/2 + \eta_2(5(v/w)/12)} \quad (4.20)$$

v is the deformation of the diametral mid section of the cylinder,

w is the normal approach of the flat plate to the center of the cylinder, or half of the total normal deformation of the cylinder.

$\lambda = \ln(4/\gamma) - 0.5$

γ is the half-angle of contact between the cylinder and the flat plate which can be calculated by the following equation

$$w/r = \frac{(\ln(4/\gamma) - 0.5)(1-\gamma^2/8 + \gamma^4/192) + (5\gamma^2/48 - 267\gamma^4/11520)}{(2/\gamma^2 - 5/8 + 67\gamma^2/288 - 475\gamma^4/24192)}$$

where r = radius of the cylinder.

$$\eta_x = \frac{\gamma^2(1-\gamma^2/6)}{4(1-\gamma^2/8+\gamma^4/192)} \quad \text{and}$$

$$\eta_\phi = \frac{\gamma^4(1-3\gamma^2/16)}{8(1-\gamma^2/8+\gamma^4/192)}$$

Values from these equations which are based on a large deformation theory, were compared to values based on the Hertz linear elastic contact theory and it was concluded that the large deformation theory was the most accurate but only by one percent.

When two cylindrical bodies, with their axes parallel, are pressed in contact by force P per unit length, they make contact over a long strip of width $2a$ lying parallel to the axis. To determine the value of a and total dimetrical compression, Hertz contact theory can be used. The assumptions made in the Hertz theory are as follows (Johnson, 1985): 1) The surfaces are continuous and non-conforming: $a \ll r$; r is the radius of the contacting body 2) The strains are small: $a \ll r$. 3) Each solid can be considered

as an elastic half-space $a \ll r$, $a \ll$ length of the cylinder, and 4) the surfaces are frictionless.

For the rhizome problem the first and third conditions are met. Johnson (1985) states that the Hertz theory is valid for some composite materials. For contact of solids where each could have surface layers whose elastic properties differ from lower layers, Hertz theory is valid as long as the top layer is large compared with the contact size 2a. Also rhizomes are composed of material similarly to that in corn cobs, and the Hertz contact theory predicted accurately the value for a (Chikwendu and Anazodo, 1984); therefore the use of the Hertz contact theory instead of a large deformation theory to predict contact compression probably would not lead to sizeable errors. Finally, although the rhizome is covered with roots which could cause friction between contacting rhizomes, Hertz theory can be used for water hyacinths because friction at the interface of two non-conforming bodies brought into normal contact plays a part only if the elastic constants of the two materials are different (Johnson, 1985). Therefore, the Hertz contact theory can be used for water hyacinths, and the following formula for total compression, δ of a rhizome diameter compressed between two other hyacinths through the mid-points of the contact areas was used

$$\delta = 2\,P\frac{(1-\nu^2)}{\pi E}\left[\ln\,(4\,r/a_1) + \ln\,(4\,r/a_2) - 1\,\right] \quad (4.20)$$

where a_i are the semi-contact-widths from Hertz contact theory given by

$$a_1^2 = 4 F r / \pi E^*$$

where E^* is the composite modulus of the two contacting cylinders or

$$E^* = \frac{1 - \nu_1^2}{E_1} + \frac{1 - \nu_2^2}{E_2}$$

<u>Materials and Methods.</u>

In this section the procedures used to determine Young's modulus and Poisson's ratio for water hyacinth rhizomes are discussed. These values will be used whenever the total diametrical compression of a rhizome is needed (Equation 4.20).

Rhizomes were collected from Biven's Arm, a lake where water hyacinths are not harvested; consequently, the rhizomes were long. Long rhizomes were collected so that long test samples could be cut. Samples were 2 to 3 cm long and 1 to 2 cm in diameter because these dimensions are typically prepared for a compression test (Sitkei, 1986). Roots were left on the rhizomes to correspond to an actual compression condition. After the samples were cut, rhizomes were observed to be rounded and covered with a soft, spongy tissue which probably represented internodal material. The internodal area produces the roots and leaves. The amount of spongy material varied from sample to sample. The samples were subjected to radial compression on an Instron universal testing machine until the rhizome cracked. Loading rates of 25, 50 and 127 cm/min were used to check viscoelastic tendencies.

Typical force-deformation behaviour of a radially compressed rhizome composite exhibits two distinct stages. During the beginning

of the test, the roots and spongy material flatten with very little resistance. This behaviour is non-linear. Then, there is a linear elastic region where the primary resistance to radial deformation is the rhizome beneath the spongy material. Unlike many biological materials, rhizomes do not have a bio-yield point, although, a definite rupture point was evident.

Young's modulus was calculated from Equation 4.19 with values of deformation and force from the linear portion of the force-deformation curve. Poisson's ratio was calculated by the method of Chikwendu and Anazodo (1984) and the experimental setup is briefly reviewed below.

Successive photographs of the cross-section of each rhizome sample were taken with a video camera during radial compression. The test ended when the sample cracked. The video was viewed frame by frame and the total lateral extension and normal compression were measured. These measurements were used to calculate Poisson's ratio by the use of Equation 4.20.

Results and Discussion

Poisson's ratio was successfully determined for two samples because other samples tended to rotate under the flat plate, which, made measurements difficult with video monitor. These two values are 0.49 and 0.45. They are considered typical for a material that approaches that of a liquid (Mohsenin, 1978). The rhizomes are 90 percent water, therefore, these values are expected. Hence, the average value, 0.47, was used in the calculations of Young's modulus.

The Young's modulus ranged from 7.5 to 11 MPa with an average of 9.9 MPa (Table 4.2). Loading rate appeared to have no effect on these values. The magnitude of the modulus was between those for corn cob

(18 MPa) and Russet burbank potato (4.4 MPa) (Chikwendu and Anazodo 1984, and Mohsenin, 1978).

Further, the force per length of rhizome at the transitional point of the force-deformation curve ranged from 20 to 40 N/cm. As was mentioned earlier, this force corresponds to the force required to flatten the roots against the rhizomes. From the data, the roots approximately projected 0.5 cm upward from the rhizomes.

4.3.4 Summary

Poisson's ratio was determined to be 0.47 and the apparent Young's modulus, 9.9 MPa. The force required to flatten roots against a rhizome is between 20 and 40 Newtons per meter of rhizome length. An equation was presented that could predict the compressive forces involved when rhizomes contact.

Table 4.2 Experimental values of apparent Young's modulus of water hyacinth rhizomes.

Loading velocity cm/min	Young's modulus MPa
25	10.6
25	9.9
25	8.1
50	11.3
50	10.6
50	7.8
127	11.1
127	9.7
127	10.6
Average	9.9
Standard deviation	±1.3

CHAPTER V
MATHEMATICAL MODEL OF WATER HYACINTHS TOWS

This chapter is concerned with development of a mathematical model of a water hyacinth towing system. It is based on physical laws that elements of the system and their interconnections obey. Principal system variables are mat horizontal velocity and displacement. Using towing velocity as the input, the model was solved numerically, and calculated values of towing force and mat compaction were compared to experimental data. Further, in this chapter the physical condition of the system prior to vertical displacement or 'roll under" is described.

Conceptual Model

To construct an accurate mathematical statement of components and their interconnections, knowledge of the structure of the system is required. At the beginning of this study, physical components of a water hyacinth mat and their interconnections were obscure and ill defined. So the pattern of different component interconnections was manipulated until the resulting mathematical model generated accurate input-output relationships for different boundary and input conditions. The resulting conceptual model of a mechanical system that consists of a water hyacinth mat of length L and width W and a device that encloses them is shown in Figure 5.0. The distance from

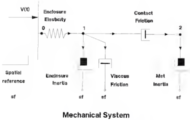

Figure 5.0 Conceptual model of a water hyacinth mat inside of a moving frame

node 1 to node 2 is the length L of the mat, hence, node 1 represents the rear of a mat, and node 2, its front end.

The enclosing device is analogous to the test equipment used in the towing experiments described in Chapter 4.0. For other towing devices, different kinds and arrangement of elements could model the enclosure. It is represented by a spring and a mass element. The spring (representing the cantilever beams on the towing test apparatus) is connected to a frame of finite mass which surrounds a mat.

The water hyacinths are represented by two types of friction elements and a mass element. One of the friction elements is associated with viscous friction of the water hyacinths moving through the water. As the system begins to move, motion is imparted first to its rear. It is for that reason that the viscous friction element is positioned at node 1. The other, connected between nodes 1 and 2, is associated with sliding friction of contacting petioles.

Initially the system is at rest. At time $t > 0$, the enclosure moves at velocity $V_B(t)$. As the mat begins to move, it compacts. When compaction ends, the entire mat moves uniformly at the speed of the enclosure device.

Element Descriptions

Mass elements. To represent part of a physical system by an ideal translational mass, it is necessary that all of the particles be connected together and that they move with substantially equal or proportional velocities and accelerations (Shearer et al., 1971). The constitutive equation for an ideal mass element is derived from Newton's second law, and inertial force F_M equals

$$F_{M_i} = M_i \frac{dV_i}{dt} \qquad (5.0)$$

where, i denotes node number

M_1 = mass of the enclosure = M_e

M_2 = mass of water hyacinth mat plus mass of water accelerated with the mat = M_m

V_i = Velocity a water hyacinth mat at node i with respect to spatial reference

Water mass is added to that of the water hyacinth mat, because it gives the additional force required to accelerate the mass of fluid set in motion by the acceleration of the plant parts submerged in the water. The additional amount of water mass depends on the shape of the moving object (Gerhart and Gross, 1985). Water hyacinth rhizomes, the principal objects in flow, are similar to circular cylinders. For circular cylinders in two-dimensional flow, the apparent increase in mass due to water equals the mass of fluid displaced by the circular cylinders (Prandtl and Tietjens, 1934).

Spring element. Any mechanical element that undergoes a change in shape when subjected to a force can be characterized by a stiffness element, provided that an algebraic relationship exists between the elongation or compression and the force. The cantilever beams used in the towing experiments can be idealized as one stiffness element. For a linear cantilever, elastic force F_k equals

$$F_k = K \; X_{01} \qquad (5.1)$$

where K is an elastic constant and X_{01} equals the cantilever deflection that is given by

$$X_{01} = X_0 - X_1$$

where X_0 is the displacement of the towing device and X_1 is the displacement of a water hyacinth mat at node 1. Also, the rest deflection is defined to be zero, with $X_0 - X_1 = 0$, and no force applied to the cantilever.

For small deflections, δ, of a cantilever beam, K can be calculated as follows:

$$K = \frac{P}{\delta} = \frac{3\ E\ I}{\ell^3} \tag{5.2}$$

Where P = concentrated load at free end of beam,

ℓ = beam length,

E = modulus of elasticity,

I = moment of inertia = $\frac{b\ h^3}{12}$

b = beam width, and

h = beam thickness.

For b = 5 cm, h = 0.3175 cm, ℓ = 0.30 m, and E (for steel) = 2.07×10^{11} Pa. K is 3,000 N/m. The experimental towing device had four cantilevers beams acting conjunctively so the theoretical value of K is 12,000 N/m.

Another useful property of the idealized enclosure device is its natural frequency, ω_n, in rad/s given by

$$\omega_n = \left[\frac{K}{M_e}\right]^{\frac{1}{2}} \tag{5.3}$$

The period of vibration of a undamped enclosure device depends on the mass of enclosing device M_e and on K of its cantilever beams, and is independent of magnitude of oscillations. For an enclosure mass equal to 12.0 kg and K equal to 12 000 n/m the system natural frequency is 5 hz.

Viscous element. Drag friction is primarily due to the presence of water hyacinth rhizomes. If, in addition, the enclosure device is equipped with objects that protrude into the water, different types of viscious elements may have to be added to the model. In Chapter 4, the description of drag due to rhizomes was found to be a nonlinear function of mat velocity. In the conceptual model, mat velocity is the velocity of node i. Therefore, the steady flow description of the viscous element is

$$D_f = 1000\ N_p\ A_r\ C_d\ V_i\ |V_i| \qquad (5.4)$$

The absolute value symbol is required to change direction of force with change in direction of velocity. Drag coefficient for steady flow was found to be $C_d = 0.4436 \exp(0.306 \frac{W}{L})$ (Equation 4.18).

Drag on a mat in unsteady flow was not determined experimentally, because several physical components in the system were simultaneously active (e.g. inertia, drag, and contact friction elements), and drag coefficient is not known. When a bluff body starting from rest moves through a fluid, wakes and vortices form and change with time. Viscous drag is proportional to the rate of increase of energy resulting from the lengthening of these wakes (Panton, 1984). Also, the drag coefficient of a group of spherically shaped particles moving

with acceleration in a turbulent fluid was found to be functions of particle Reynolds number and degree of turbulence, but not of the acceleration (Kiker and Ross 1966 and Torobin and Gauvin 1961). Therefore, the value of C_d in steady flow can not be used in Equation 5-4 while a mat is accelerating, because the towing experiments and theory described in the previous chapter give a precise mathematical description of drag only when the rate of increase of wakes is constant, or when the effects of system acceleration are absent. Therefore, an expression for C_d that is valid for unsteady flow conditions was obtained through model simulation.

Contact friction. Another friction force arises because plants can be connected to each other through entanglement of petioles, a condition that occurs when the population density is high and when the plants are healthy and have not been attacked by insects or disease. Amount of petiole entanglement is measured by connectivity (see Chapter 3). When entangled petioles slide against each other during relative motion, friction resists that motion. As a water hyacinth mat compacts, petioles slide over each other. A film of liquid exists between these petioles, because leaves are wet. If the resulting fluid flow is laminar, the following describes the contact sliding force F_c:

$$F_c = B_L V_{12} \qquad (5\text{-}5)$$

where $V_{12} = V_1 - V_2$; variables V_1 and V_2 correspond respectively to horizontal velocities of the front and back ends of a water

hyacinth mat with respect to a spatial reference and B_L is the interactive plant friction coefficient, which is proportional to the contact area and the water viscosity and inversely proportional to the thickness of the film (Close and Fredrick 1978). Parameter B_L was evaluated through simulation.

Model Formulation

In this section, a set of equations were developed that described a water hyacinth towing system. First, node equations are written; then, a set of state variables equations is derived, and finally, a set of output equations is derived from the state variables.

Node equations. The system model has two nodes; therefore, two vertex equations describe force interactions at these nodes. Applying Newton's third law, the sum of the forces at these nodes must equal zero. The node equations are

Node	Equation	
1	$-F_k + F_{M_e} + D_f + F_e = 0$	(5.6)
2	$-F_e + F_{M_n} = 0$	(5.7)

State variable equations. A set of state variables describes completely the behavior of a system in response to its inputs. Therefore, knowledge of their values at reference time t_0 and the values of the inputs for all $t \geq t_0$ is sufficient for evaluation of state and output variables of the system for all $t \geq t_0$ (Close and Federick, 1978). One state variable is usually associated with each energy storage element (e.g. inertia and spring elements). For this study, the state variables are X_{31}, V_1 and V_2. The former pertains to cantilever deflection and variables V_1 and V_2 correspond respectively to horizontal velocities of the front and

back ends of a water hyacinth mat with respect to a spatial reference. To derive state variable equations, an expression for the derivative of each state variable is formulated in terms of other state variables, time, and inputs by using nodal equations and component descriptions. The description used for the rate of change of X_{e1} is derived below, and it is in terms of input variable V_2 and state variable V_1.

$$\frac{dX_{e1}}{dt} = \frac{d(X_2 - X_1)}{dt} = V_2 - V_1 \qquad (5.8)$$

The state variable equation for V_1 was derived in the following way. First, the time derivative of V_1 was expressed by using the component description of the inertia of the enclosure device (Equation 5.0).

$$\frac{dV_1}{dt} = F_{M_e}/M_e \qquad (5.9)$$

Next, another expression for F_{M_e} was found since a state variable equation is in terms of other state variables. It was obtained from nodal equation 5.6, and substituted into Equation 5.9.

$$\frac{dV_1}{dt} = (F_K - D_f - F_c)/M_e \qquad (5.10)$$

Finally, the second state variable equation was obtained after appropiate component descriptions were substituted into Equation 5.10.

$$\frac{dV_1}{dt} = [K\, X_{e1} - 1000.0\, N_p\, A_r\, C_d\, V_1 |V_1| - B_L(V_1 - V_2)]/M_e \qquad (5.11)$$

The final state variable equation (Equation 5.10) was derived in a similar fashion:

$$\frac{dV_2}{dt} = F_{M_m} / M_m = F_c / M_m$$
$$= [B_L (V_1 - V_2)] / M_m \qquad (5.12)$$

<u>Output equations.</u> Mat compaction, towing force, sliding contact force and drag force are output variables of the model of interest, and they are calculated at any time, t, from the state variables. Sliding contact and drag force are computed from Equations 5.4 and 5.5. Mat compaction for a mat of original length L is computed from:

$$\text{Mat compaction} = L - (X_2 - X_1) \qquad (5.13)$$

where X_1 and X_2 are calculated after the following equations are integrated:

$$\frac{dX_1}{dt} = V_2 \qquad (5.14)$$

$$\frac{dX_2}{dt} = V_2 \qquad (5.15)$$

Towing force is calculated:

$$\text{Towing force} = K (X_{01}) \qquad (5.16)$$

<u>Method of Solution and Parameter Estimation</u>

Equations 5.8, 5.11 and 5.12 are a system of coupled first-order differential equations, one of which is nonlinear. They represent a water hyacinth towing system. The system was solved to determine ways to reduce the towing force, study mechanisms of "roll under" and mat compaction, and determine parameters C_d of unsteady flow conditions and B_L.

To solve the equations, initial conditions, estimates of parameters, V_0 as a function of time, and numerical integration were needed. System variables and outputs were evaluated numerically because one of the equations was nonlinear and two parameters were unknown. The initial conditions were needed to compute state and some output variables. At t_0, V_1 and V_2 were always set at zero. Displacement of the spring element was zero ($X_0 = X_1 = 0$) and X_2 equaled L. Further, at $t \geq t_0$, velocity V_0 was a function of time, and system variables and outputs were evaluated numerically until the system reached steady state or until the derivatives of the state variables were zero.

The fourth-order Runge-Kutta formula was used to solve the equations in a "problem solver" program written in Turbo-Pascal (Appendix A). The program utilizes a published version of Runge-Kutta (Press et al., 1986). The step size, based on accuracy, was 0.02 seconds for an integration interval of 15 seconds.

To estimate the parameters B_L and C_d, the following scheme was adopted. The program accepted estimates for parameters B_L and C_d, solved the differential equations, and returned values of towing force and mat compaction at specified times. Output values were compared to experimental values that were generated during the unsteady part of the towing experiments discussed in Chapter 4. This procedure for parameter estimation was repeated until correlation between calculated and experimental data was better than 80%. Towing force on mats like those described in towing experiments 4 through 7 (Table 4.0) was calculated. Plants in the mats ranged from very small to big-

Initial estimations of parameters C_d and B_L were based on some prior information. For instance, the drag coefficient in unsteady flow conditions was assumed to equal the experimental value for steady flow conditions at large t. The other parameter, B_L, was thought to be constant because physical factors that could effect it do not vary appreciably in a water hyacinth mat. Friction coefficient B_L is known to be proportional to contact area and viscosity and inversely proportional to film thickness. In water hyacinths, film thickness and viscosity do not vary and contact area probably varies slightly as a mat moves.

Results of Parameter Estimation and Model Analysis

Parameter values. Correlation coefficients between model and experimental data for six different conditions ranged from 0.86 to 0.98 (Table 5.0). The lower coefficients were associated with experimental and calculated towing force compared at t = 1 s. This was partly due to uncertainty of the exact time a experiment started (i.e. the beginning of an experiment was defined to be the time of the first nonzero data point recorded by the data logger). Also, too few data points were obtained because experimental data were recorded every second (i.e. large sampling time).

Expressions describing B_L and C_d selected on the basis of these correlations (Table 5.0) were found to depend on plant size and other physical characteristics of a mat. Further, drag coefficient was found to vary with X_1 until steady conditions were reached, and it is described by the following equation:

$$C_d = 0.4436 \exp(0.906 \frac{W}{L'}) \qquad (5.16)$$

where

$$L = D_v + X_1 \qquad \text{for } V_2 < V_1$$

$$L' = L \qquad \text{for } V_2 = V_1$$

where D_v is a constant. This expression supports the concepts that a mat moves at constant speed when both the front and back ends move at the same velocity, and the unsteady drag coefficient of a mat changes to its steady flow value.

Table 5.0 Correlation coefficient between model and experimental towing force

Sample size L x W	Towing velocity m/s	Number of data points	r^2
1.83 m x 1.22 m	0.90	9	0.98
— — —	0.14	9	0.95
	0.21	9	0.93
0.61 m x 1.22 m	0.15	5	0.86
1.22 m x 1.22 m	0.15	9	0.96
2.44 m x 1.22 m	0.15	9	0.97

The constant D_v was necessary because without it C_d would not have a finite value at small values of X_1. Constant D_v was determined to be 0.5 for three of the experiments modelled, and it equaled 0.35 for a mat that was comprised of large plants and large rhizomes with long roots (Table 5.1). The experiment number there represents the towing experiment modelled. This constant determines the value of the drag coefficient just as a mat starts from rest. As the value of D_v decreases in different types of mats, the drag

coefficient increases. Therefore, it is conceivable that very long roots and large rhizomes would effect it. In addition, D_v was not affected by mat geometry or towing velocity.

Table 5.1. Values of B_L and D_v of the mats modelled.

B_L	D_v	Experiment modelled	Average plant length, cm
30.0	0.50	5	25.0
145.0	0.48	4	61.0
178.0	0.50	7	71.0
140.0	0.35	6	93.0

The values of B_L determined for each mat modelled is presented in Table 5.1. It was affected by the type and condition of the plants that comprised a mat but it was unaffected by mat geometry or towing speed. The mat with the lowest value of B_L (30) was comprised of very small plants. The friction factor of mats of larger plants varied from 140 to 178. This range of values could be due to connectivity. Small plants were connected primarily by stolons, and larger plants were connected primarily by overlapping leaves.

Effect of towing velocity. Mats were accelerated experimentally in one of two ways. For towing velocities less than 0.25 m/s, the acceleration resembled a step velocity input, and for towing velocities ≥ 0.25 m/s, the mats were accelerated incrementally to offset possible detrimental inertial effects on the testing equipment.

The following describes model response to a single step velocity input. When a mat was towed, towing force increased very quickly and then decreased gradually to a steady value. The maximum value occured independently of mat area at approximately 0.1 s, because inertia due to the mass of the enclosure is the principal active component on the system up to that time which was expected because the natural frequency of the spring - enclosure system was 5 hz. As speed increased and mat length increased, it took longer for the force to decrease to a steady value (Figures 5.1 and 5.2). For a sample size 2.44 m long by 1.22 m wide, time to reach steady conditions ranged from 2 s for a velocity of 0.9 m/s to 10 s for a velocity of 0.2 m/s.

Sliding friction (Equation 5.4) and viscous friction (Equation 5.5) are responsible for damping (Figure 5.3). Viscous friction increases as the square of velocity; so, as towing velocity increases, it quickly becomes the principal active component.

Mat compaction as measured at steady state, increased linearly with towing velocity. When B_L equaled 30, compaction of a 2.44 m long x 1.22 m wide a mat increased with towing velocity according to this expression:

$$\text{mat compaction} = 1.43 * V_o$$

To offset the effects of inertia of the enclosure, mats were accelerated incrementally whenever the desired final towing velocity was greater than 0.25 m/s. Increments varied according to the discretion of the trolley operator. Velocity inputs to the problem solver were changed incrementally with time in an attempt to mimic these experiments. Two simulations were done: one involved a mat with very small plants, the other involved medium-sized plants typical of a

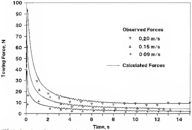

Figure 5.2 Effect of towing velocity on a 2.44 m long x 1.22 m wide mat that was comprised of medium-sized plants averaging 61.0 cm in length. Fluctuations are due to numerical instabilities related to V_{12}

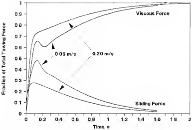

Figure 5.3 Effect of towing velocity and drag on a mat. The mat measured 2.44 m in length and 1.22 m in width. It was comprised of medium-sized plants averaging 61.0 cm in length.

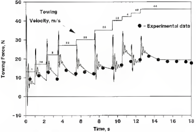

Figure 5.4 Towing force on a 2.44 m long x 1.22 m wide mat accelerated incrementally. The mat was comprised of small plants averaging 25.0 cm in length.

water treatment system. The former is presented in Figure 5.4. Experimental data showed that the model accurately predicted the increase in towing force with towing velocity. The model predicted that every time velocity was incremented, there would be a peak in the towing force due to the inertia of the enclosure device, and that the friction forces generated by the plants were not great enough to immediately affect the oscillatory response of the combined spring - mass components. However, these predicted peaks in the towing force were not evident in the experimental data. This could have been due to the sparseness of experimental data in these regions. Also, the model used a step velocity increment, and in practice, step inputs are nearly impossible to obtain.

On the other hand, a set comprised of larger plants had friction forces large enough to dampen quickly the combined response of spring-mass components (Figure 5.5). Peak force due to inertia of the enclosure was predicted by the model, but was not evident in the experimental data, although, the model accurately predicted the general increase in towing force. This discrepancy probably was related to the practical impossibility of a step velocity input.

The advantage of reducing inertial effects through a slow increase in towing velocity is that the maximum towing force can be reduced by a factor of four (Figures 5.5 and 5.6). The "problem solver" program can be used to model the response of the system to other kinds of velocity inputs. Different ramp velocity inputs were modelled (Figure 5.7), and results indicate that inertial forces could be negligible for small accelerations.

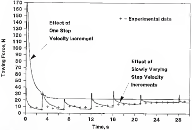

Figure 5.5 Differences in towing force on a 2.44 m long x 1.22 m wide mat due to the way it was accelerated to 0.33 m/s. Experimental data was obtained from a test where the mat was comprised of medium-sized plants averaging 61.0 cm in length.

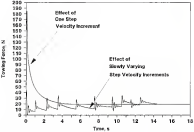

Figure 5.6 Differences in towing forces on a mat due to the way it was accelerated to 0.44 m/s. Mat conditions and velocity steps are identical to those in Figure 5.4.

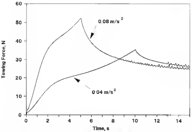

Figure 5.7 Top curve represents force respond on a 2.44 m long x 1.22 m wide mat comprised of large plants that was given a ramp velocity input to acheive a final towing velocity of 0.4 m/s in 5 s. Bottom curve represents respond due to a slower acceleration where final towing velocity was reached in 10 s.

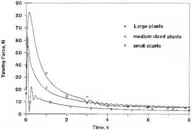

Figure 5.8 Effect of plant size on towing force. Mat areas were 2.44 m long by 1.2[illegible] m wide and towing velocity was 0.15 m/s.

Effect of mat characteristics. The effect plant size has on towing force is evident in Figure 5.8. Small plants (population density, 206/m^2) have small rhizomes, and although the total number of plants in a mat is large, the total projected area in flow is small compared to the expected total area from a mat of larger plants. Therefore, as depicted in Figure 5.8, the viscous force at low towing velocities on small rhizomes was not large enough to dampen quickly the oscilatory response of the combined spring-mass components. In contrast, oscilatory response was not evident in mats comprised of large plants.

Also, initial oscilatory response of spring-mass components takes longer to dampen (Figure 5.9) if mats are small. As the width of the mat decreased, sliding force contributed a greater proportion of the total force on the system, and mat compaction (%) decreased (Figures 5.10 and 5.11; Table 5.2). Compaction of a 1.22 m long by 0.61 m wide mat was approximately half the compaction of a 1.22 m long by 1.22 m wide mat. On the other hand, as the initial length of the mat decreased, mat compaction (%) increased slightly.

Table 5.2. Theoretical effects of mat size on compaction. The mats were towed at approximately 0.15 m/s, and were comprised of medium-sized plants averaging 61.0 cm in length.

Sample Size L X W	Compaction %	Initial Areal Mass Density kg/m^2
1.22 m x 0.61 m	1.39	21.3
1.22 m x 1.22 m	2.70	19.0
2.44 m x 1.22 m	2.25	16.9

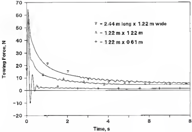

Figure 5.9 Towing force on different sizes of mats towed at 0.15 m/s. Mats were comprised of medium-sized plants averaging 61.0 cm in length

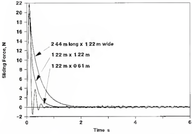

Figure 5.10 Contact friction force due to petiole sliding over each other on different sizes of mats towed at 0.15 m/s. Mats were comprised of medium-sized plants averaging 61.0 cm in length

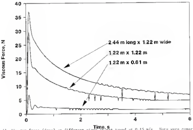

Figure 5.11 Viscous force (drag) on different sizes of mat towed at 0.15 m/s. Mats were comprised of medium-sized plants averaging 61.0 cm in length.

Physical description of "roll under". Buoyancy acts through the centroid of a displaced volume and this centroid changes position if the body tips. While a water hyacinth is vertical due to support by other plants or by floats, its centroid of displaced volume is positioned near the center of its rhizome, and its center of gravity lies above the centroid of displaced volume. These conditions make water hyacinths unstable vertically (Gerhart and Gross, 1985). Plants submerge if enough force is applied to overcome the buoyant force or if the plants are tipped so that their metacenters lie below their centers of gravity. Metacenter is defined as the intersection of the buoyant force and centerline of the volume of the object.

The buoyant force of a mat was described in chapter 3. Buoyant force per unit mat area depends on areal biomass density and on the physical condition of the plants. If plants are well connected, force above the normal buoyancy force is required to submerge a mat due to the support structure of a mat. Mats towed in this study entered the water at velocities exceeding 0.40 m/s, although, one mat was stable up to 1 m/s. This mat was prevented from compaction, and its leading edge was not free to rotate. In general, the velocity when "roll under" occurred ranged between 0.4 and 0.6 m/s. Calculations indicated that mats towed in this study required from 173 to 300 Pa to submerge them (e.g., a 3 m^2 mat required over 500 N to submerge it).

Observations indicated that mats comprised of different sized plants and connectivities become unstable at different values of compaction. For instance, a mat consisting of small plants became unstable when compaction was approximately 32 %, and mats consisting of larger plants became unstable when compaction was approximately

10%. These compaction data were independent of sample size if the mat was comprised of plants of the same size and areal density.

One of the assumptions made in the development of the model was that a mat compacts until the rhizomes touch (Chapter 4). This implies compaction of approximately 90%. After observing that mats consistently "roll under" at lower compaction, the model was changed to allow for the formation of bridges in a mat (i.e. enough rhizomes are in contact within the mat to prevent further compaction). To determine the system response when rhizomes are in contact, another element was added to the conceptual model representing the elastic nature of rhizomes in contact. It is described as follows:

$$\text{Elastic contact of rhizomes} = K_r\ (\ L + (\ X_1 - X_2\ ) - D_c\ )$$

where D_c equals the maximum expected compaction of a given mat, and $K_r = 10 \times 10^{10}$ Pa. The elastic constant K_r is the elastic modulus of rhizomes calculated in Chapter 4. This element was positioned in parallel with the contact friction element. With the addition of this element, Equations 5.11 and 5.12 changed to:

$$\frac{dV_1}{d\ t} = [K\ X_{01} - 1000\ N_p\ A_r\ C_d\ V_1 |V_1| - B_L(V_1 - V_2) - K_r\ (\ L + (\ X_1 - X_2\ ) - D_c)]/M_c \qquad (5.17)$$

$$\frac{dV_2}{d\ t} = [B_L\ (\ V_1 - V_2\ ) + K_r\ (\ L + (\ X_1 - X_2\ ) - D_c)]\ /M_m \qquad (5.18)$$

These expressions were solved by the "problem solver" program. Results showed that when compaction equaled D_c, towing forces per

unit mat area exceeded 200 Pa. This force was sufficient to submerge mats provided that the plants contact at an angle and a vertical elastic contact force is produced. This is illustrated in Figure 5.12. Observations showed that plants were tipped and touching at "roll under". Model output beyond "roll under" were considered meaningless because the program solves only one dimensional problems. Furthermore, calculated towing velocity at " roll under " were within 10% of the experimental values.

Summary

-Mats of water hyacinths towed within a rectangular enclosure were modelled. The model consisted of two inertial elements, one for the mat and one for the enclosure, a contact friction element, a viscous friction element, an elastic element for the enclosure, and an elastic element for rhizome contact.

-Some of the parameters required to solve the model were estimated from comparison of experimental and computer simulation data.

- The model accurately predicted towing force and compaction for different sizes and types of mats and velocity inputs.

- A method to predict when a mat becomes unstable was presented.

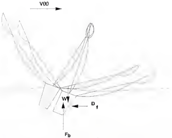

Figure 5.12 Pictorial representation of a plant starting to "roll under". The shaded plant comes into contact with the unshaded plant that is free to rotate. A vertical force due to this contact permits rotation. Buoyancy is F_b, drag is D_f, and plant weight is W. Each plant normally has 5 to 6 leaves. Plants are in unstable equilibrium because their center of mass is above the center of buoyancy.

CHAPTER VI
MAT COMPACTION MODEL

The model of a water hyacinth mat presented in Chapter 5 was used to determine the response of a mat constrained at one end to compaction from the opposite end. Calculated compressive force was compared with experimental data. This information was be used to determine the capacity of towing devices and to design more efficient removal devices.

Conceptual Model

The conceptual model of a water hyacinth mat of length L and width W inside a compressive frame is pictured in Figure 6.0. In this model, the same components developed in Chapter 5 are used to represent the water hyacinth mat. The compressive frame represents the test equipment used to compact mats, so data obtained from experiments could be used to validate the mat model. The mat was situated between two bars, a front pusher bar and a fixed rear bar. The front bar pushing the mat was considered rigid; therefore, only its mass is represented. The back bar, on the other hand, has a elastic contact element attached to it, which represents interaction between rhizomes and the rear bar.

Initially the system is at rest. The distance from node 0 to node 1 is the rest length of the mat. As the front bar moves at

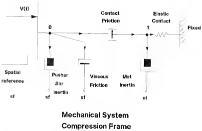

Figure 6.0 Conceptual model of water hyacinths subjected to compaction.

velocity V_0 it compresses the mat against the back bar, and the mat shortens. Compaction continues until the plants "roll under."

Model Formulation.

The element descriptions were given in Chapter 5. Newton's third law applied at node 1 produces the following equation:

$$F_{M_m} - F_s + F_{K_b} = 0 \qquad (6.0)$$

where

$$F_{M_m} = M_m \frac{d\,V_1}{d\,t} \qquad (6.1),$$

$$F_s = B_L\,(\,V_0 - V_1\,) \qquad (6.2)$$

and

$$F_{K_b} = K_b\,(\,X_1 - L\,) \qquad (6.3)$$

Force F_{K_b} is the elastic contact force of plants against the fixed bar, and it equals zero when $X_1 = L$. Rest length of the mat is L, and X_1 is deformation of spring at node 1. Elastic constant $K_b = 2 \times 10^7$ N/m which equals approximately the inverse of the composite modulus of elasticity of the two contacting bodies (rhizome and steel rear bar) multiplied by mat width W. The state variable equations are

$$\frac{d\,X_1}{d\,t} = V_1 \qquad (6.4)$$

$$\frac{d\,V_1}{d\,t} = [\,B_L\,(\,V_0 - V_1\,) - K_b\,(\,X_1 - L\,)\,]/M_m \qquad (6.5)$$

The output equations were chosen to describe mat compaction and total compressive force. Compressive force was calculated at node 0 from input variables and computed state variables for time $t \geq t_0$

Compressive Force =

$$= M_{e} \frac{d V_0}{d t} + 1000 N_p A_r C_d V_0^2 + B_L (V_0 - V_1) \qquad (6.6)$$

where

$$\frac{d V_0}{d t} = \text{constant for a ramp velocity input}$$

Mat compaction was calculated on the basis of the change in specific area because specific area compensates for differences in initial areal standing densities of mats. Specific area A_s is defined by:

$$A_s = A_t / N_p \qquad (6.7)$$

where N_p equal the mass of the plants within the frame and A_t equals the area within the compressive frame at time t:

$$A_t = (L - X_0) W$$

where X_0 was obtained after the integration of $V_0 = \frac{d X_0}{d t}$

Method of Solution and Parameter Estimation

Equations 6.4 and 6.5 represent a system of coupled first-order differential equations. Together with the output equations, they represent compaction of a water hyacinth mat. The equations were solved to determine the behavior of a mat subjected to different compaction velocities, mechanisms of "roll under", and parameters B_L

and C_d of unsteady flow conditions The latter were studied because their descriptions were not presumed equal to those for mat tows.

To facilitate the estimation process and to solve the system equations, the fourth-order Runge-Kutta formula was used, and a problem solver routine was written that calculated values of mat compaction and compressive force every 0.013 s (Appendix B). Initial conditions were $V_c = 0$, $X_1 = L$ and $X_0 = 0$. Input velocity was a function of time and it was specified to be a ramp in the first 2 s and a constant after $t > 2$ s. Ramp descriptions were

Type 1 Acceleration

$$V(t) = \frac{V_s}{0.2}\, t \qquad \text{for } t \leq 0.2 \text{ s and}$$

$$V(t) = V_s \qquad \text{for } t > 0.2 \text{ s}$$

Type 2 Acceleration

$$V(t) = \frac{V_s}{0.5}\, t \qquad \text{for } t \leq 0.2 \text{ s and}$$

$$V(t) = V_s \qquad \text{for } t > 0.2 \text{ s}$$

where V_s was the steady compaction velocity. These velocity inputs were chosen because they modelled accurately the experimental compaction velocity. For one experiment, however, type 2 acceleration was used to attempt to produce a better correlation between experimental and calculated compressive force.

Parameters B_L and C_d for towing were obtained in Chapter 5; however, the boundary conditions of a towed mat are different from those in compaction. In compaction, mats are forced to compact. Contact area changes greatly and, therefore, contact friction coefficient B_L should too. Also, drag coefficient of a mat during unsteady towing need not be the same as for compaction. Therefore, parameters C_d and B_L were estimated for compaction. The "problem solver" accepted estimates for these parameters, solved the equations, and returned values of towing force and mat compaction as functions of time. The compressive force was compared with experimental values. This procedure for parameter estimation was repeated until acceptable correlation ($r^2 > 0.8$) between calculated and experimental data of mats for different plant size and different compaction velocity was acheived.

Initial estimations of parameters C_d and B_L were based on some prior information. Initially, B_L was held constant since it was found to be a constant in Chapter 5, and C_d was assumed to vary as a mat compacted. Because drag coefficient for steady flow conditions drag coefficient was determined to be a function of mat geometry (Equation 4.18), and because the dominant characteristic of a mat in compaction is reduced mat length, C_d was initially varied according to a variation of Equation 4.18

$$C_d = 0.4436 \exp(0.906 \frac{W}{L-X_s}) \qquad (6.6)$$

Experimental Compression Tests

A test rig was designed and constructed for this investigation. The 3 m by 3 m compression frame (Figure 6.1) consisted of a rake moving along a pair of tubular rails and a similar fixed rake. Rake tines on 20 cm centers extended 30 cm below the rake tube and 38 cm above. The moving rake weighed 23.1 kg, and it was driven by chains on each rail which, in turn, were driven by a hydraulic motor or a modified automotive winch. With these devices four different constant compaction velocities could be obtained: approximately 0.05 m/s, 0.12 m/s, 0.28 m/s and 0.4 m/s.

Force and motion were transmitted from the chain to the rake through a rake support carriage equipped with load cells to measure force and parallel linkages. Signals from the load cells and from position sensing potentiometer were recorded on a Campbell Scientific CR7 data logger equipped with "Burst mode" software which allowed a sampling interval of 0.2 s.

Tests were conducted on plants at the following locations: IFAS field laboratory, Zellwood, Fl; IFAS Swine Research Unit, UF; and Walt Disney World Sewage plant, Kissimmee, Fl. After the mat was compacted (Figure 6.2), seven plants were characterized by shoot height, root length, mass, petiole mass, number of petioles and total length. All plants inside of the frame were weighed, and the weight was divided by the area of the frame in order to determine standing area densities. Rhizome length and population density were calculated using the expressions presented in Chapter 3. Mat buoyancy and connectivity were measured in some experiments, and estimated for others.

Figure 4.1 Compression frame was equipped with a sliding bar and load cells located at both ends of the bar. As the bar moved toward the fixed end bar, the mat compacted.

Figure 6.2 A water hyacinth mat was being compacted

Compression tests were performed on 15 different mats and characteristics of five of these mats are presented in Table 6.0. Many mats were compacted to test the model under different conditions of compaction velocity, connectivity, areal density, plant size and acceleration, and to test the equipment. These five mats were sufficient for parameter estimation.

Table 6.0. Characteristics of mats compacted

Experiment	N_p	M_p kg	A_r m^2	Total length, m	Observations
1	1610	237.0	0.003	0.85	well connected
2	1700	156.1	0.0006	0.33	
3	1600	90.0	0.00025	0.23	open spaces
4	2826	177.0	0.00022	0.27	
5	2610	130.0	0.0008	0.22	sickly

Before a compaction experiment started, a grid of nylon cord was placed on top of the mat. The grid was used to determine when "roll under" occurred because it begins when grid lines bunch closely together. All experiments were videotaped. After the tapes were viewed, the position of the moving rake at "roll under" was recorded.

Results and Discussion

Experimental observations. Reported observations pertain to force compaction behavior, "roll under" and kinematics. Compaction experiments indicated that as compaction velocity increased, the relationship between compressive force and compaction changed. At low velocity (< 0.15 m/s), the relation between compressive force and specific area was approximately linear up to "roll under". At higher velocity (> 0.25 m/s), the relation was obviously nonlinear. The

position within a mat where instability or "roll under" occurred appeared to be the most dense area of the mat, and therefore, it occurred at different locations within different mats. Generally if plants were well connected, grid lines up to the start of "roll under" moved at the same speed. In contrast, towing experiments showed that motion was imparted first to the rear of a mat when the mat started from rest.

<u>Parameter determination</u>. Parameters C_d and B_L varied as a mat compacted. Also, B_L decreased with increasing compaction velocity and connectivity. The drag coefficient followed the relation given by Equation 6.8, which was further evidence supporting the mat drag coefficient developed in Chapter 4.0.

On the other hand, B_L was found not to be a constant, as it was in the towing model, but to increase with displacement of the pusher bar. Friction coefficients vary proportionally with contact area (Close and Frederick, 1978). Since water hyacinth contact area increased with pusher bar displacement and plant population, the following equation was deduced:

$$B_L = \bar{B}_L N_p X_o \qquad (6.9)$$

where $\bar{B}_L$ is a constant. After this expression was substituted into the model, calculated and experimental compressive force agreed (Table 6.1). Correlation coefficients ranged from 0.93 to 0.99. The one experiment where agreement was not strong ($r^2 = 0.51$) will be discussed later.

Table 6.1 Contact friction coefficient and other variables used in the simulations of mat compaction

Exp #	Compaction velocity m/s	$B_L' N_p$	Roll Under position mat compaction %	Pusher bar acceleration type[1]	Correlation between experiment and model r^2
4	0.053	11745	21	1	0.98
2	0.13	7065	30	1	0.97
5	0.12	4515	21	1	0.96
5	0.26	209	21	2	0.93
1	0.40	153	43	1	0.99
3	0.40	32	44	1	0.51

[1] See text for explanation

Friction coefficient B_L decreased with compaction velocity and connectivity (Table 6.1). Plants in experiments 3 and 5 were of low connectivity, and plants in experiments 1, 2 and 4 were healthy and highly connected. Friction coefficients of different mats compacted at the same velocity was always significantly lower in mats of lower connectivity. Friction coefficient of well connected mats decreased linearly with compaction velocity, and the regression relation follows ($r^2 = 0.96$)

$$\frac{B_L}{X_u} = 12415 - 3132.4\, V_u$$

Too few data points were available to obtain a regression equation for mats of low connectivity, however, B_L of these mats ranged from 30% to 60% of those of highly connected mats. Also, for compaction

velocities exceeding 0.26 m/s. B_L approached the values obtained from towing experiments.

An explanation for B_L as a function of velocity can be found in Chapter 5, mat compaction increased linearly with towing velocity until "roll under". This implies that a mat reaches a maximum compaction and "roils under" without need for a rear restraint if mat velocity is high enough. During compaction experiments, however, "roll under" in a mat is acheived at lower compaction velocity by restraining it and forcing it to compact. Therefore, extra friction force is required at low compaction velocities to compact a mat until "roll under", and it is reflected in a larger friction coefficient.

System behavior and mechanisms of "roll under". At low compaction velocity, the fraction of total compressive force due to contact friction was great, at higher velocities, it was small. Graphs of experimental data showed that at low compaction velocity the relation between compressive force and specific area (Figures 6.3 and 6.4) was linear. Calculated drag indicated that it does not dominate at velocity below 0.15 m/s, but it becomes dominate very quickly above 0.15 m/s. At the same time, contact force becomes less important (Figures 6.5 - 6.6).

In general, compressive force increases as compaction velocity increases (Figure 6.6). The model could not accurately predict compressive force in a mat that consisted initially of many open spaces (Figure 6.9). Connectivity is considered to be zero in these cases. Furthermore, inertia of the moving bar caused a rapid increase in compressive forces at the beginning of compaction (Figures 6.5 and

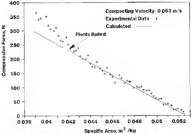

Figure 6.3 At low compacting velocity and before plant "roll under", compressive force consists primarily of contact friction. Friction coefficient increases linearly as a mat compacts.

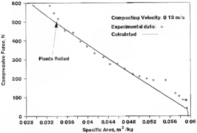

Figure 6 4 At this velocity, the principal force was due to contact friction forces. Friction coefficient decreases as velocity increases.

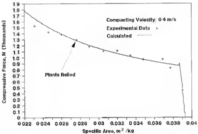

Figure 6.5 At this velocity, compressive force is primarily due to drag. The increase in Force at 0.04 m^2/kg specific area is due to inertia of the compression bar.

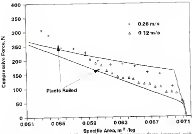

Figure 6.6 A mat was compacted twice at different velocities. Compressive force increased with velocity.

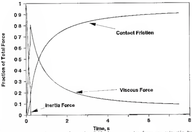

Figure 6.7 When compaction velocity was lower than 0.15 m/s, compressive force was primarily due to contact friction. Inertia was due to the compression bar.

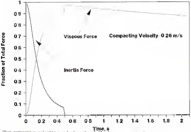

Figure 6 3 When compaction velocity was higher than 0 25 m/s, compressive force was due primarily to viscious friction (drag). Inertia was due to the compression bar. Contact force was not a major component

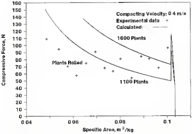

Figure 6.9 The mat consisted of few plants and many open spaces. The model was not accurate with these conditions. Curves represent two computer simulations, one with 1600 plants and the other with 1100 plants

6 6), because the mass element representing the mass of the compressive bar was the principal active component of the system

Compaction (%) at "roll under" varied according to plant population and plant length Generally, it decreased as population increased and average plant length decreased Root length was not a factor since all plants tested had short roots "Roll under" occurred between 20 and 40% compaction, which was higher than the values in towing tests "Roll under" occurred at the front end of a mat during towing tests but inside the mat during compaction tests Therefore plants were naturally supportive in compaction, making it more difficult for them to enter the water Compressive force on a mat of large plants was large enough to submerge the mat, provided the plants were tipped to create the required vertical force component Except with mats of large plants, "roll under" was usually accompanied by a large increase in compressive force

Summary

-A mathematical model was developed to predict the response of a water hyacinth mat to forced compaction Initially unknown parameters, C_d and B_L were estimated through comparison of calculated and experimental compressive force Friction coefficient varied with compaction velocity, compaction, and connectivity Drag coefficient varied with the change in length of a mat

-The model for mat compaction accurately predicted compressive force "Roll under" can be predicted on a basis of compaction or buoyancy

-Compressive force was dominated by drag at velocity exceeding 0 26 m/s and by contact force at velocity below 0 15 m/s

-Compressive force increased with compaction velocity

-Compaction (%) at "roll under" ranged from 20 to 40% and it decreased with increasing plant population and decreasing average plant length. It was not affected by compaction velocity.

CHAPTER VII
CONCLUSIONS AND RECOMMENDATIONS FOR FURTHER RESEARCH

Water hyacinth mats were described quantitatively in terms of plant mass, areal density, mat buoyancy, connectivity, and rhizome length. These physical characteristics were parameters in hydromechanical models describing (1) a mat towing and (2) a mat in forced compaction. Critical physical properties distinguishing one mat from another are average plant length, standing density, and average plant mass.

To develop any hydromechanical model, a relation between drag and velocity is required. Newton's drag law was used to describe this relationship for a mat. In this case, area in the direction of flow is projected area of the total number of rhizomes. Drag coefficient is independent of Reynolds number, and it is related nonlinearly to mat geometry. A higher drag coefficient is associated with higher width-to-length ratio.

A mat compacts when it is towed or forced against a barrier. Generally, for compaction between 20 and 40% (Computed (length/L)100) rhizomes compress together, and elastic forces are generated. By the use of large deformation theory, elastic properties of rhizomes were

obtained. Poisson's ratio and Young's modulus were determined, respectively, to be 0.47 and 9.9 MPa.

Conceptual models were developed to describe machine water hyacinth interactions for two different harvesting operations, rectangular mat towing and forced compaction. Mass and elastic elements of test machinery, petiole contact friction element, mass element of a mat, mat viscous element and rhizome elastic compressive element were components of these machine water hyacinth systems. Their descriptions and interconnections were based on experimental observations and physical and hydromechanical properties. The equations derived from the conceptual model were solved numerically using a Runge-Kutta integration method to study system behavior in response to velocity input. Output variables such as towing or compaction force and mat compaction were predicted over time with good correlation with experimental data. Mat instability or "roll under" was found to occur at a specific mat compaction.

As a tool for the design of better harvesters, the model could be used to determine:

-Optimal towing and compaction conditions for different harvesting schemes and

-Effect of different acceleration patterns

-Power and energy requirements of different designs.

The design of equipment, such as conveyors, rakes, removal devices, and restraining barriers, could be based on the following hydromechanical information from this research:

-Slowing accelerating a mat and moving machine parts to reach a constant velocity saves energy. Because the highest forces in

the systems studied were due to inertia, plants should be kept moving at constant velocity

-Drag force is reduced by towing long, narrow mats.

-"Roll under" is prevented by maintaining appropriate plant density and operating speed.

-Compacting a mat to decrease its drag coefficient could save towing costs.

Additional research should be done for large scale verification and application of the model. Moreover, model parameters connectivity and petiole friction coefficient could be investigated to determine an empirical relation between the two parameters. Dependency of this coefficient on other plant characteristics could be clarified, too. Also, because C_d was determined only for rectangular mats, drag coefficient could be determined for other mat geometries. Furthermore, development of the "problem solver" into a software program with input and output screens is needed for user convenience.

Finally, the movement only of a mat and moving machine parts was investigated. Study of water flow under a moving mat, which is a very complicated problem, could describe mat movement due to negative acceleration.

Appendix A
Problem Solver Program

Listing of MODELS3 PAS page 1

```
PROGRAM d15r2(input,output)
(* driver for routine RKDUMB *)
uses crt
CONST
   nvar=4
   nstep=750;
TYPE
   float = extended
   glnarray = ARRAY [1  nvar] OF float,
VAR
   i,j  count  index  integer
   x1 x2 Vel El, Np. M. Ar. Trial constant constant1 constant2
     Compare  Length vert1, Width
     distance distancet,distance1 distance11
     distance2 distance3 distance4 distance5
     distance6  distance7  distance8   float
   vstart   glnarray
   xx   ARRAY [1  2000] OF float
   Force   ARRay [1  2000] of float
   y   ARRAY [1  nvar] OF float,
   E   ARRAY [1  nvar] OF float
    fout   text
(*$I MODFILE PAS *)
>     TYPE
>        char12 = string[12],
>     FUNCTION sngl(x float) float,
>     BEGIN
>        sngl  := x
>     END
>     PROCEDURE glopen(VAR infile text  filename char12)
>     BEGIN
>        assign(infile filename)
>        reset(infile)
>     END
PROCEDURE derive(x   float  y   glnarray,deltat float,
       VAR dydx   glnarray)
(* The arrays y and dydx must carry the dimension given to
them in the calling routine  *)
BEGIN
         {distance1:=y[1],} compare :=y[1],{    end
   if ( x >= 1 00  ) and ( x < 2 250 ) then  begin
        vel :=0 15
        compare := y[1]-distance1
        distance2 :=compare
          end,
   if ( x>=2 25)  and (x < 3 5) then  begin
        vel :=0 200
        compare :=y[1]-distance2,
        distance3 :=compare
        end
        if ( x>=3 50) and (x < 5 5) then begin
```

Listing of MODEL53 PAS, page 2

```
        vel =0 25
        compare =y[1]-distance3,
        distance4 =compare
        end
        if ( x>=5 5) and (x < 7 50) then begin
        vel =0 280
        compare =y[1]-distance4
        distance5 =compare
        end
        if ( x>=7 5) and (x < 9 45) then begin
        vel =0 33,
        compare =y[1]-distance5
        distance5 =compare
        end
        if  (x >=9 45) and ( x< 10 5) then begin
          vel =0 380
          compare =y[1]-distance4
          distance5 =compare
          end
        if (x >=10 5) and (x < 11 5) then begin
          vel =0 40
          compare =y[1]-distance6
          distance7 =compare
          end
          if (x >=11 5) and (x < 12 5) then begin
          vel =0 420
          compare =y[1]-distance7,
          distance8 =compare
          and )
      constant1 =12000 0
       if ((length-(y[3]-y[1])) > 0 880) then constant2 =10e6
         else constant2 =0 0
      b1 =140 0
      constant =0 350
     distancet =distance+deltat*vel,
    if ((y[4]-y[2])<0 0035)
     and (y[4] >0 0) and (y[4] >= y[2]) or
       ( constant >length )
      then distance11 =length else
        distance11 =compare+constant
     trial =Np*Ar*0 4245*exp(0 933*width/distance11)*abs(y[2])*y[2]
   dydx[1]  =y[2]
   dydx[2]  = 1 0/12 0*(-constant1*(y[1]-distancet)
            +b1*(y[4]-y[2])-trial-constant2*(length+(y[1]-y[3])-0 88))
   dydx[3] =y[4]
  dydx[4] =1 0/m*(-b1*(y[4]-y[2])+constant2*(length+(y[1]-y[3])-0 88));

END
(*$I RK4 PAS *)
> PROCEDURE rk4(y dydx  glnarray, n  integer, x h  real delta float
>               VAR yout  glnarray)
> (* Programs using routine RK4 must provide a
> PROCEDURE derivs(x real  y glnarray  VAR dydx glnarray),
```

Listing of MODEL53 PAS-include file RK4 PAS, page 3

```
> which returns the derivatives dydx at location x
> given both x and the function values y  The calling program
> must also define the types
> TYPE
>    glnarray = ARRAY [1..nvar] OF real
> where nvar is the number of variables y. *)
> VAR
>    i  integer;
>    xh hh h6  real
>    dym dyt yt  glnarray
> BEGIN
>    hh := h*0.5;
>    h6 := h/6.0;
>    xh := x+hh;
>    FOR i := 1 to n DO BEGIN
>       yt[i] := y[i]+hh*dydx[i])    END
>    derivs(xh,yt,delta+hh dyt);
>    FOR i := 1 to n DO BEGIN
>       yt[i] := y[i]+hh*dyt[i])    END
>    derivs(xh,yt,delta+hh dym)
>    FOR i := 1 to n DO BEGIN
>       yt[i] := y[i]+h*dym[i]
>       dym[i] := dyt[i]+dym[i]
>    END
>    derivs(x+h,yt,delta+h dyt);
>    FOR i := 1 to n DO BEGIN
>       yout[i] := y[i]+h6*(dydx[i]+dyt[i]+2.0*dym[i])
>    END
> END;
(*$I RKDUMB.PAS *)
> PROCEDURE rkdumb(vstart glnarray; nvar: integer; x1,x2: float;
>                  nstep: integer);
> (* Programs using routine RKDUMB must provide a
> PROCEDURE derivs(x float; v glnarray; VAR dvdx glnarray)
> which returns the derivatives dvdx at location x  given
> both x and the function values v  They must also define the type
> TYPE
>    glnarray = ARRAY [1..nvar] OF float
> where nvar is the number of functions  They must also
> declare the variables VAR  xx  ARRAY [1..250] OF float
> y  ARRAY [1..nvar,1..250] OF float, in the main routine  *)
> VAR
>    kount,k,i: integer;
>    x h delta  float
>    v,vout,dv: glnarray;
> BEGIN
>    FOR i := 1 to nvar DO BEGIN
>       v[i] := vstart[i];
>    END
>    force[1] :=0.0
>    xx[1] := x1;
>    writeln(fout,xx[1]:6:3,'  ',v[1]:8:3,'  ',force[1]:7:2,'  '
```

Listing of MODEL53 PAS-include file RKDUMB5 PAS, page 4

```
>              v[2] 5 3, ' '. distance 6 3, ' ', v[3] 6 3, '
>                ',0 0,  ',(length v[3]+v[1]) 6 3
>              ,' ',vel 5 3,  ' trial 6 2}
>
>    x  = x1,
>    h  = (x2-x1)/nstep
>    delta =0 0,
>    FOR k  = 1 to nstep DO BEGIN
>       derive(x,v delta dv)
>       rk4(v dv nvar x,h delta vout),
>       IF (x+h = x) THEN BEGIN
>          writeln('pause in routine RKDUMB')
>          writeln( stepsize to small ), readln
>       END
>       x  = x+h,
>       xx[k+1]  = x,
>
>       FOR i  = 1 to nvar DO BEGIN
>          v[i]  = vout[i]
>
>       END
>  {if x < 1 0 then  begin vel =0 11
>  end;
>    if ( x >= 1 D0  ) and ( x < 2 250 ) then  begin
>         vel =0 15
>
>
>           end,
>
>    if ( x>=2 25)  and (x < 3 5) then  begin
>         vel =0 200
>        end,
>         if ( x>=3 5) and (x < 5 50) then begin
>         vel =0 250
>        end,
>         if  (x >=5 50 ) and ( x< 7 50) then vel =0 28
>         if  (x >=7 5 ) and ( x< 9 45) then vel =0 33
>         if (x >=9 45 ) and ( x < 10 5 ) then vel =0 38
>         if (x >=10 5 ) and ( x < 11 5 ) then vel =0 40
>         if (x >=11 5 ) and ( x < 12 5 ) then vel =0 42
>         if x >=12 5 then vel =0 480    }
> if ((v[4]-v[2])<0 0035) and (v[4]>0 0)
>       and (v[4] >v[2]) or ( constant >length)
>      then distance11 =length else
>        distance11 =v[1]+constant
>
>   trial =Mp*Ar*0 4245*exp(0 933*width/distance11)*abs(v[2])*v[2]
>
>
> distance =distance+vel*h
>
>  {output variables, remove the brackets around fout to write to
file}
```

Listing of MODEL53.PAS-include file RKDUMB5.PAS page 5

```
>    Force[K+1]:=constant1*(distance-v[1]);
>     writeln((fout,)xx[K+1]:6:3,' ',v[1]:6:3,' ', force[K+1]:7:2,' ',
>                 v[2]:5:3,' ', distance:6:3,' ', v[3]:6:3,' ',
>                 v[4]:5:3,' ', bl*(v[2]-v[4]):6:3,'
',(length-v[3]+v[1]):6:3
>                 ,vel:5:3,' ',trial:6:2);
>
>    END
> END;

BEGIN
            assign(fout,'ba4h815.prn');
   rewrite(fout);
   clrScr;
   vert1:=25.0;
    x1 := 0.00;
                    vel:=0.150;
   distance:=vel*x1;
   distance11:=0.0;
   distancet:=0.0;
   distancel:=0.0;
   count:=1;
   repeat
   vstart[count]:= 0.0;
   Inc(count);
  until (count>Nvar);
                    vstart[3]:=2.44;

   Np:=74.0;
   Ar:=0.0040*1000.0;
   M:= 52.09+(np*3.14*Ar*0.025/4.0);
   Length:=2.44;
   Width:=1.22;
   trial:=0.0;
   x2 := 15.0;
   compare:=0.0;
   rkdumb(vstart,nvar,x1,x2,nstep);
   {close output data file}
   flush(fout);
   close(fout);
END
```

Appendix B
Problem Solver Program
For Compaction Characteristics

Listing of MODELVAL.PAS, page 1 at 31/08/88

```
PROGRAM d15r2(input,output);
(* driver for routine RKDUMB *)
uses crt;
CONST
   nvar=2;
   nstep=300;
TYPE
   float = extended;
   glnarray = ARRAY [1..nvar] OF float;
VAR
   i,j, count, index : integer;
   x1,x2,Vs1,Si, Np, M, Ar, Trial,
     constant,constant1,constant2,
     Compare, Length,vert1, Width,
     distance,distancet,distancei,distanceii,
     distance2,distance3,distance4,distance5,
     distance6, distance7, distance8 : float;
   vstart : glnarray;
   xx : ARRAY [1..2000] OF float;
   Force : ARRay [1..2000] of float;
   y : ARRAY [1..nvar] OF float;
   B : ARRAY [1..nvar] OF float;
   fout
    : text;
(*$I MODFILE.PAS *)
>     TYPE
>        char12 = string[12];
>
>     FUNCTION sngl(x:float):float;
>     BEGIN
>        sngl := x
>     END;
>
>     PROCEDURE glopen(VAR infile:text; filename:char12);
>     BEGIN
>        assign(infile,filename);
>        reset(infile)
>     END;
PROCEDURE derivs(x : float; y : glnarray;deltat:float;
       VAR dydx : glnarray);
(* The arrays y and dydx must carry the dimension given to
them in the calling routine. *)
BEGIN
 if ( x <= 0.2) then vel :=0.6*x else
     vel :=0.120 ;
      compare :=y[1];
      distancet :=distance+deltat*vel;
      if ((distancet+y[1]-length) >=1.65)
          then constant2 :=10e6
        else constant2 :=0.0;
        constant :=1.70*np;
```

```
     b1 =constant*distancet
       dydx[1] =y[2]
  dydx[2] =1 0/m*(b1*(vel-y[2])-
             constant2*(distancet+y[1]-length+1 65)
             -200000 0*(y[1]-3 048)).
END
(*$I RK4 PAS *)
> PROCEDURE rk4(y dydx  glnarray  n  integer, x,h  real delta float,
>              VAR yout  glnarray)
> {* Programs using routine RK4 must provide a
> PROCEDURE derivs(x real, y glnarray  VAR dydx glnarray)
> which returns the derivatives dydx at location x,
> given both x and the function values y  The calling program
> must also define the types
> TYPE
>    glnarray = ARRAY [1  nvar] OF real
> where nvar is the number of variables y  *)
> VAR
>    i  integer
>    xh hh h6  real
>    dym,dyt yt  glnarray
> BEGIN
>    hh  = h*0 5
>    h6  = h/6 0
>    xh  = x+hh
>    FOR i  = 1 to n DO BEGIN
>       yt[i]  = y[i]+hh*dydx[i]
>    END
>    derivs(xh,yt,delta+hh dyt)
>    FOR i  = 1 to n DO BEGIN
>       yt[i]  = y[i]+hh*dyt[i]
>    END
>    derivs(xh yt delta+hh dym).
>    FOR i  = 1 to n DO BEGIN
>       yt[i]  = y[i]+h*dym[i].
>       dym[i]  = dyt[i]+dym[i]
>    END
>    derivs(x+h yt delta+h dyt).
>    FOR i  = 1 to n DO BEGIN
>       yout[i] := y[i]+h6*(dydx[i]+dyt[i]+2 0*dym[i])
>    END
> END
(*$I rkDUMBv7 PAS *)
> PROCEDURE rkdumb(vstart glnarray  nvar  integer
>           x1 x2  float  nstep  integer)
> (* Programs using routine RKDUMB must provide a
> PROCEDURE derivs(x float  v glnarray  VAR dvdx glnarray)
> which returns the derivatives dvdx at location x
> given both x and the function values v
> They must also define the type
> TYPE
```

Listing of MODELVAL PAS-include file RKDUMBV7 PAS, page 3

```
>    glnarray = ARRAY [1  nvar] OF float
> where nvar is the number of functions  They must also
> declare the variables
> VAR
>    xx  ARRAY [1  250] OF float
>    y  ARRAY [1  nvar,1  250] OF float.
> in the main routine  *)
> VAR
>    kount,k,l: Integer,
>    x h delta veln  olength acel  float
>    v vout,dv. glnarray.
> BEGIN
>    FOR i  = 1 to nvar DO BEGIN
>       v[i]  = vstart[i]
>    END
>    force[1] =0 0,
> veln =vel,
>    xx[1]  = x1,
>    writeln(fout xx[1] 6 3  ' ,v[1] 6 3,' ', force[1] 7 2
>          v[2] 5 3  ', distance 6 3     0 0
>          (length*width/(m-(np*3 14*Ar*0 025/4 0))) 6:4
>                 vel 5 3    trial 6 2).
>    x  = x1
>    h  = (x2-x1)/nstep
>    delta =0 0
>    FOR k  = 1 to nstep DO BEGIN
>       derive(x,v delta dv)
>       rk4(v dv nvar x h delta vout).
>       IF (x+h - x) THEN BEGIN
>          writeln( pause in routine RKDUMB )
>          writeln( stepsize to small ), readln
>       END
>       x  = x+h,
>       xx[k+1]  = x,
>          FOR i  = 1 to nvar DO BEGIN
>          v[i]  = vout[i]
>         END,
>       if (x <= 0 2) then begin vel:=0 60*x
>          acel =0 60  end else
>          begin
>         vel =0 120
>         acel =0 0
>         end
>         distance:=distance+vel*h
>         nlength =length-distance
>            compare =distance
>            bl =distance*constant
>          distancell =nlength
>          trial =Np*Ar*0 44436*exp(0 906*width/distancell)*vel*vel
>          if (trial>vertl) or (bl*(vel-v[2]) >vertl) then  begin
>           writeln(xx[k+1]     , Rolled Under )
```

Listing of MODELVAL PAS-include file RKDUMBV7 PAS page 4

```
>            halt
>          end,
>       Force[K+1] =21 3*accel+trial+b1*(vel-v[2])+
>                     constant2*(distance+v[1]-length+1 50)
>     writeln({fout }xx[K+1] 6 3,'  ',v[1] 6 3,'  ', force[K+1] 7 2,
>               '  ', v[2] 5 3,'  ', distance 6 3
>             ,b1*(vel-v[2]) 6 3   '
>           (nlength*width/(m-(np*3 14*Ar*0 025/4 0))) 6 4
>           '  ',vel 5 3,  ',trial 6 2),
>    END
> END
BEGIN
                        assign(fout, 's501872 prn'),
   rewrite(fout),
   clrScr,
   vertl =2000 0
    x1  = 0 00
                          vel =0 12,
   distance =vel*x1
   distancell =0 0
   distancet =0 0 ,
   distancel =0 0
   count =1
   repeat
   vstart[count]  = 0 0,
   inc(count),
  until (count>Nvar);
                        vstart[1] =3 048,
   Np =2610 0
   Ar =0 0009*1000 0
   M = 130 2+(np*3 14*Ar*0 025/4 0)
   Length =3 048
   Width =3 048
   trial =0 0
   x2  =15 0000
   compare =0 0
   rkdumb(vstart,nvar,x1,x2,nstep),
   {close output data file}
   flush(fout),
   close(fout)
END
```

REFERENCES

Amazodo, U G N 1983 Mechanical Properties of the Corn Cob Under Quasi-static Radial Compression Trans of the ASAE 26(4) 1222-1228

Amazodo U G and S C Chikwendu 1983 Poisson's Ratio and Elastic Modulus of Radially Compressed Biomaterials I Small Deformation Approximation Trans of the ASAE 26(3) 923-929

Bagnall L O, C E Schertz, and D M Dubbe 1987 Harvesting and Handling of Biomass In K R Reddy and W H Smith Aquatic Plants for Water Treatment and Resource Recovery Magnolia Publishing Inc Orlando pp 599-620

Benedict, B A 1985 Fluid Mechanics Class notes University of Florida Gainesville FL

Bogart D M 1949 The Effects of Aquatic Weeds on Flow in Everglades Canals Proc Soil Sci of FL 9:32-52

Chikwendu U and C N Amazodo 1984 Poisson's Ratio and Elastic Modulus of Radially Compressed Biomaterials - II Large Deformation Approximation Trans of the ASAE 27(5) 1563-1572

Close, C M and D K Frederick 1978 Modeling and Analysis of Dynamic Systems Houghton Mifflin Company Boston

Culpepper, M M and J L Decell 1978 Mechanical Harvesting of Aquatic Plants Tech Rep A-78-3 Rep 1 Vol 1 U S Army Engineer Waterways Expt Station Vicksburg MS

Debusk T A and F Dierber 1984 Effect of Nitrogen and Fiber Content on the Decomposition of the Water Hyacinth Hydrobiologia 118(2) 199-204

Gerhart P M and M J Cross 1985 Fundamentals of Fluid Mechanics Addison-Wesley Publishing Company Reading

Grimison N 1937 Correlation and Utilization of New Data on Flow Resistance and Heat Transfer for Cross Flow of Gases Over Tube Banks Trans of the ASME 59(8) 583-594

Herschy, R W 1978 Accuracy Hydrometry Principles and Practice John Wiley and Sons London

Johnson, K L 1985 Contact Mechanics Cambridge University Press New York

Kahn A 1980 Movement of Floating Plants Under Natural Forces In P A Smith Mechanical Harvesting of Aquatic Plants- Rep 2 A-78-3 Evaluation of Selected Handling Functions of Mechanical Control (Appendix C) U S Army Engineer Waterways Expt Station Vicksburg MS pp 1-121

Kays, W M and A L London 1984 Compact Heat Exchangers McGraw Hill Book Company New York

Kiker C F and I J Ross 1966 An Equation of Motion for Multiple Granular Particles in Free Fall in Enclosed Vertical Ducts Trans of ASAE 9(4) 468-473, 479

Knipling S H West and W T Haller 1971 Growth Characteristics, Yield Potential and Nutritive Content of Water Hyacinths Proc of the Soil and Crop Sci Soc of Florida (USA) 30 51-63

Kouwen N A and R Li 1980 Biomechanics of Vegetative Channel Linings J Hydr Div ASCE, 106(6) 1085-1103

Kouwen, N N Li, and D Simons 1981 Flow Resistance in Vegetated Waterways Trans of the ASAE 24(3) 684-90

Kouwen N A , R Li and D B Simons 1980 A Stability Criteria for Vegetated Waterways Intern Symp Urban Storm Runoff Lexington KY pp 203-10

Kouwen N A and T E Unny 1973 Flexible Roughness in Open Channels J Hydr Div ASCE, 99(HY5) 713-28

Kouwen, N A T E Unny and H M Hill 1969 Flow Retardance in Vegetated Channels J of the Irr and Drain Div ASCE 95(IR2) 329-42

Lamb Sir H 1945 Hydrodynamics Dover Publications New York

Lencastre, A 1987 Handbook of Hydraulic Engineering Ellis Horwood Limited Chichester

Mallory T H Chiang E Cutter and E Gifford Jr 1970 Sequence and Pattern of Lateral Root Formation in Five Selected Species Amer J Bot 57(7) 800-809

McQuiston, F C and G D Parker 1982 Heating Ventilating and Air Conditioning Analysis and Design John Wiley and Sons Inc New York

Mohsenin, N N 1978 Physical Properties of Plant and Animal Materials Gordon and Breach Science Publishers New York

Panton, R. L. 1984. Incompressible Flow. John Wiley and Sons, Inc. New York.

Penfound, W. and T. Earle. 1948. Biology of the Water Hyacinth. Ecol. Monogr. 18:447-472.

Petryk, S. and G. Bosmajian III. 1975. Analysis of Flow Through Vegetation. J. of the Hydr. Div. ASCE. 101(HY7):871-884.

Powell, K. E. 1978. Weed Growth – a Factor of Channel Roughness. In W. W. Herschy. Hydrometry: Principles and Practice. J. Wiley and Sons. London.

Powell, R. W. 1946. Flow in a Channel of Definite roughness. Trans. of ASCE 111:531-566.

Prandtl, L. and O. G. Tietjens. 1934. Applied Hydro- and Aeromechanics. Dover Publications, Inc. New York.

Press, W. H., B. P. Flannery, S. A. Teukolsky, and W. T. Vetterling. 1986. Numerical Recipes. Press Syndicate of the University of Cambridge. New York.

Ramey, V., Ed. 1987. Aquaphyte. 7(2):11.

Ranz, W. E. 1952. Friction and Transfer Coefficients for Single Particles and Packed Beds. Chemical Engineering Progress 48:247-253.

Reddy, K. R. 1988. Water Hyacinth Cropping Systems: I. Production. In W. H. Smith and J. R. Frank. Methane from Biomass: a Systems Approach. Elsevier Applied Science. London. pp. 103-158.

Ree, W. O. and V. J. Palmer. 1949. Flow of Water in Channels Protected by Vegetative Linings. Technical Bulletin No. 967. U. S. Dept. of Agriculture. Washington, D. C. 115 pp.

Roa, P. S. 1920. The Formation of Leaf-bladders in *Eichhornia speciosa*, Kunth (Water Hyacinth). Ind. Bot. Soc. J. 1:219-225.

Sayre, W. W. and M. L. Albertson. 1961. Roughness Spacing in Rigid Open channels. J. of the Hydr. Div. ASCE. 87(HY3):121-150.

Schardt, J. D. 1986. The 1986 Florida Aquatic Plant Survey. Bureau of Aquatic Plant Management. Tallahassee.

Schlichting, H. 1979. Boundary-Layer Theory. McGraw Hill Book Company. New York.

Shearer, J. L., A. T. Murphy and H. H. Richardson. 1971. Introduction to System Dynamics. Addison-Wesley Publishing Company. Reading.

Shih, S. F. and C. S. Rahi. 1982. Seasonal Variations of Manning's Roughness Coefficient in a Subtropical Marsh. Trans. of the ASAE 25(1):116-119.

Sitkei, G 1986 Mechanics of Agricultural Materials Elsevier New York

Steel, R and J H Torrie 1960 Principles and Procedures of Statistics McGraw-Hill Book Company, Inc New York

Stephens N E, B D Blackburn, D E Seaman, and L W Weldon 1963 Flow Retardance by Channel Weeds and Their Control J of the Irr and Drain Div ASCE 89(IR2) 31-47

Stickler, A 1929 Beitrage zur Frage der Geschwindigheits Formel und der Rauhigkeit-zahlen fur Strome, Kanale und Geschlossene Leitungen Mitteilungen des Eidgenossischer Amtes fur Wasserwirtschaft No 16g Bern, Switzerland Tarnopolskii, Y M and T Kincis 1981 Static Test Methods for Composites Van Nostrand Reinhold Company New York

Torobin, L B and W H Gauvin 1961 The Drag Coefficients of Single Spheres Moving in Steady and Accelerated Motion in a Turbulent Fluid American Institute of Chemical Eng 7:615-619

Tucker, C S 1981 Relationships Between Culture Density and the Composition of Three Floating Aquatic Macrophytes Hydrobiologia 85 73-76

Turner, Q K and N Chanmeesri 1984 Shallow Flow of Water Through Non-submerged Vegetation Agricultural Water Management 8(4) 374

Zamora, C V, U Chiancharden and N Laodan 1982 Morpho-anatomical Studies of Eichhornia crassipes(mart) Solms Water Hyacinth Geographic Distribution Nat Appl Sci Bull 32 1-41

BIOGRAPHICAL SKETCH

Rayann Jean Petrell was born in Grand Forks, North Dakota. She moved while still in primary school to Eveleth, Minnesota. There, she graduated from high school in 1972. At the University of Minnesota Duluth, she received in 1975 a B.A. degree in biology. The Pennsylvania State University awarded her a M.S. degree in agricultural engineering in 1977.

Before she started graduate studies at the University of Florida, she worked for several years in Mexico. There, she worked on projects in the areas of physical properties, project engineering and development, and food engineering. She became interested in aquatic plant culture as an alternative to conventional sewage treatment. It was that interest that brought her to the University of Florida for graduate studies.

I certify that I have read this study and that in my opinion it conforms to acceptable standards of scholarly presentation and is fully adequate, in scope and quality, as a dissertation for the degree of Doctor of Philosophy.

J. Wayne Mishoe, Chairman
Professor of Agricultural Engineering

I certify that I have read this study and that in my opinion it conforms to acceptable standards of scholarly presentation and is fully adequate, in scope and quality, as a dissertation for the degree of Doctor of Philosophy.

Larry O. Bagnall, Cochair
Professor of Agricultural Engineering

I certify that I have read this study and that in my opinion it conforms to acceptable standards of scholarly presentation and is fully adequate, in scope and quality, as a dissertation for the degree of Doctor of Philosophy.

Glen H. Smerage
Associate Professor of Agricultural Engineering

I certify that I have read this study and that in my opinion it conforms to acceptable standards of scholarly presentation and is fully adequate, in scope and quality, as a dissertation for the degree of Doctor of Philosophy.

Del Hatcher
Professor of Agricultural Engineering

I certify that I have read this study and that in my opinion it conforms to acceptable standards of scholarly presentation and is fully adequate, in scope and quality, as a dissertation for the degree of Doctor of Philosophy.

Chang-Yuan Sun

Chang T. Sun
Professor of Engineering Science

This dissertation was submitted to the Graduate Faculty of the College of Engineering and to the Graduate school and was accepted as partial fulfillment of the requirements for the degree of Doctor of Philosophy

December 1988

Hubert A. Bevis

Dean, College of Engineering

Dean, Graduate School